

Examining the roles of core and local temperature on forearm skin blood flow

Matthew M. Mallette, B.Kin (Hons.)

Submitted in partial fulfillment of the requirements for the degree
Master of Science in Applied Health Sciences
(Kinesiology)

Faculty of Applied Health Sciences, Brock University
St. Catharines, ON

© Matthew Mallette, 2015

ABSTRACT

The interaction between local and reflexive control of skin blood flow (SkBF) is unclear. This thesis isolated the roles of rectal (T_{re}) and local (T_{loc}) temperature on forearm SkBF regulation at normal and elevated body temperatures, and to investigate the interaction between local and reflexive SkBF control. While either normothermic ($T_{re} \sim 37.0^{\circ}\text{C}$) or hyperthermic ($\Delta T_{re} +1.1^{\circ}\text{C}$), SkBF was assessed on the dorsal aspect of each forearm in 10 participants while T_{loc} was manipulated in an A-B-A-B fashion between neutral (33.0°C) and hot (38.5°C). Finally, local heating to 44°C was performed to elicit maximal SkBF. Data are presented as a percentage of maximal cutaneous vascular conductance (CVC), calculated as laser-Doppler flux divided by mean arterial pressure. T_{loc} manipulations performed during normothermia had significantly greater effects on CVC than during hyperthermia. The decreased modification to SkBF from the T_{loc} changes during hyperthermia suggests that strong reflexive vasodilation attenuates local SkBF control mechanisms.

ACKNOWLEDGEMENTS

I would like to first thank my supervisor and mentor, Dr. Stephen Cheung. Without your supervision and guidance over the past two years, this project would not have seen the light of day. You have provided me with more support, guidance, assistance, and hours than any student could have asked for. Your passion towards your work, the witty humour you brought to every meeting, and your excellence as a researcher have made these past two years more enjoyable than I could have imagined. I look forward to many more two-wheeled lab meetings.

Secondly, I want to thank Dr. Gary Hodges for all the time spent helping this project get off the ground, teaching me how to collect and analyse skin blood flow data, being there for data collection, and helping me through the times where I thought things would never work. I am happy that over the past two years, I not only gained a colleague, but also gained a true friend.

To my lab-mates in the Environmental Ergonomics Laboratory: Geoff Hartley, Greg McGarr, Phil Wallace, Nico Coletta, Cody Watson, and Tharms Tharmaratnam, thank you for all the time spent piloting, data collecting, and letting me vent when needed. I especially want to thank Greg McGarr for assisting me with data collection, bouncing ideas back-and-forth, and helping with virtually every aspect of this thesis.

To my friends and family who have supported me over the last two years, thank you. The support that you have provided me with has been amazing. I cannot express enough gratitude for being there when I needed to vent, or forcing me to take the night off when I needed to relax.

Finally, to my mom and dad, the words written on this page cannot begin to do justice for what you have helped me accomplish. Choosing what passion I wanted to pursue was the hardest decision I have ever had to make, and I cannot begin to thank you enough for helping me through those difficult times. Thank you for your financial support that has enabled me to pursue every goal I have ever dreamt of. You have and will always be the greatest support network I could ever ask for, and I hope that one day I can return the favour for everything that you have done for me.

TABLE OF CONTENTS

ABSTRACT	II
ACKNOWLEDGEMENTS	III
LIST OF TABLES	VII
LIST OF FIGURES	VIII
LIST OF ABBREVIATIONS	IX
CHAPTER ONE: INTRODUCTION	1
CHAPTER TWO: LITERATURE REVIEW	4
2.1 DRUGS USED FOR ASSESSMENT OF SKIN BLOOD FLOW	5
2.2 METHODS TO INTRODUCE DRUGS INTO SKIN MICROVASCULATURE	8
2.2.1 MICRODIALYSIS	8
2.2.2 IONTOPHORESIS	10
2.3 SKIN BLOOD FLOW RESPONSE TO LOCAL HEATING	11
2.3.1 INITIAL PEAK	11
2.3.2 PROLONGED PLATEAU	13
2.3.3 DIE AWAY	17
2.4 SKIN BLOOD FLOW RESPONSE TO WHOLE BODY HEATING	17
2.4.1 ACTIVE HEATING	17
2.4.2 PASSIVE HEATING	18
2.5 METHODS TO MEASURE SKIN BLOOD FLOW	21
2.5.1 VENOUS OCCLUSION PLETHYSMOGRAPHY	21
2.5.2 LASER-DOPPLER FLOWMETRY	22
2.6 THERMAL BALANCE	27
2.6.1 CORE TEMPERATURE	28
2.6.2 SKIN TEMPERATURE	30
2.6.3 SKIN AND CORE TEMPERATURE INTERACTION	31
CHAPTER THREE: OBJECTIVES AND HYPOTHESIS	32
3.1 OBJECTIVES	32
3.2 HYPOTHESES	32
CHAPTER FOUR: METHODS	33
4.1 SAMPLE SIZE ESTIMATION AND PARTICIPANT CHARACTERISTICS	33
4.2 EXPERIMENTAL DESIGN	34

4.3 EXPERIMENTAL PROTOCOL	38
4.3.2 PHYSIOLOGICAL VARIABLES	40
4.4 DATA PROCESSING	40
4.5 STATISTICAL ANALYSIS	41
CHAPTER FIVE: RESULTS	43
5.1 THERMAL MANIPULATIONS	43
5.2 LOCAL TEMPERATURE EFFECTS DURING NORMOTHERMIA ON SKIN BLOOD FLOW	46
5.2.1 LASER-DOPPLER FLOWMETRY (PU)	46
5.2.2 CUTANEOUS VASCULAR CONDUCTANCE (%MAX)	46
5.3 LOCAL TEMPERATURE EFFECTS DURING HYPERTHERMIA ON SKIN BLOOD FLOW	48
5.3.1 LASER-DOPPLER FLOWMETRY (PU)	48
5.3.2 CUTANEOUS VASCULAR CONDUCTANCE (%MAX)	49
5.3.3 POLYNOMIAL CONTRASTS	50
5.4 WAVELET ANALYSIS	51
CHAPTER SIX: DISCUSSION	55
6.1 SPECTRAL ANALYSIS	59
6.2 CONCLUSIONS	60
6.3 EXPERIMENTAL CONSIDERATIONS	61
6.4 FUTURE DIRECTIONS	62
REFERENCES	64
APPENDIX A	71
APPENDIX A	75

LIST OF TABLES

TABLE 1. COMMON DRUGS USED IN SKIN BLOOD FLOW WORK.....	7
TABLE 2. FREQUENCY AND THEIR CORRESPONDING PHYSIOLOGICAL FUNCTION OF VASOMOTION. ^A THE ENDOTHELIAL BAND BROKEN UP INTO AN ENDOTHELIAL-INDEPENDENT AND -DEPENDENT ASPECT (76).	26
TABLE 3. RECTAL (T_{RE}), SKIN (\bar{T}_{SK}), CONTROL (\bar{T}_{CON}), AND EXPERIMENTAL (\bar{T}_{EXP}) ARM TEMPERATURES ($^{\circ}C$) DURING EACH MANIPULATION. EACH 'A' AND 'B' MANIPULATION WAS APPROXIMATELY 5 MIN. T_{RE} DISPLAYED IS HYPOTHETICAL DATA AS EACH PARTICIPANT BEGAN AT DIFFERENT TEMPERATURES. THE LIGHT GREY AREA IS WHEN PARTICIPANTS WERE PASSIVELY HEATED TO INCREASE T_{RE} , AND THE DARK GREY AREA IS WHEN LOCAL SKIN HEATING OCCURRED AT THE SITE OF BLOOD FLUX MEASUREMENTS WAS PERFORMED TO OBTAIN MAXIMAL FLUX VALUES.	39
TABLE 4. TEMPERATURE OF THE CONTROL (\bar{T}_{CON}) AND EXPERIMENTAL (\bar{T}_{EXP}) FOREARMS DURING LOCAL TEMPERATURE MANIPULATIONS DURING NORMOTHERMIA AND HYPERTHERMIA ($\Delta T_{RE} +1.1^{\circ}C$). SIGNIFICANT DIFFERENCES ARE WITHIN THE SAME ARM AND CORE TEMPERATURE PHASE. ^A SIGNIFICANTLY DIFFERENT THAN NORMOTHERMIC A1 ($p < 0.05$). ^B SIGNIFICANTLY DIFFERENT FROM NORMOTHERMIC B1 ($p < 0.05$). ^C SIGNIFICANTLY DIFFERENT THAN NORMOTHERMIC A2 ($p < 0.05$). ^D SIGNIFICANTLY DIFFERENT THAN HYPERTHERMIC B1 ($p < 0.05$). ^E SIGNIFICANTLY DIFFERENT THAN HYPERTHERMIC A1 ($p < 0.05$). ^F SIGNIFICANTLY DIFFERENT THAN HYPERTHERMIC B2 ($p < 0.05$).....	44
TABLE 5. LASER-DOPPLER FLOWMETRY UNITS (PU) FOR THE EXPERIMENTAL AND CONTROL ARM RESPONDING TO LOCAL TEMPERATURE CHANGES DURING NORMOTHERMIA. ^A SIGNIFICANTLY DIFFERENT FROM A1 ($p < 0.05$). ^B SIGNIFICANTLY DIFFERENT FROM B1 ($p < 0.05$). ^C SIGNIFICANTLY DIFFERENT FROM A2 ($p < 0.05$).	46
TABLE 6. CUTANEOUS VASCULAR CONDUCTANCE (CVC) EXPRESSED AS PERCENT OF MAXIMUM FOR THE EXPERIMENTAL AND CONTROL ARM DURING NORMOTHERMIA IN RESPONSE TO LOCAL TEMPERATURE MANIPULATIONS. ^A SIGNIFICANTLY DIFFERENT FROM A1 ($p < 0.05$). ^B SIGNIFICANTLY DIFFERENT FROM B1 ($p < 0.05$). ^C SIGNIFICANTLY DIFFERENT FROM A2 ($p < 0.05$).	47
TABLE 7. LASER-DOPPLER UNITS (PU) FOR THE EXPERIMENTAL AND CONTROL ARM DURING HYPERTHERMIA IN RESPONSE TO LOCAL TEMPERATURE MANIPULATIONS. ^A SIGNIFICANTLY DIFFERENT FROM B1 ($p < 0.05$). ^B SIGNIFICANTLY DIFFERENT FROM A1 ($p < 0.05$). ^C SIGNIFICANTLY DIFFERENT FROM B2 ($p < 0.05$).	49
TABLE 8. CUTANEOUS VASCULAR CONDUCTANCE (CVC) EXPRESSED AS A PERCENT OF MAXIMUM FOR THE EXPERIMENTAL AND CONTROL ARM DURING HYPERTHERMIA IN RESPONSE TO LOCAL TEMPERATURE MANIPULATIONS. ^A SIGNIFICANTLY DIFFERENT FROM B1 ($p < 0.05$). ^B SIGNIFICANTLY DIFFERENT FROM A1 ($p < 0.05$). ^C SIGNIFICANTLY DIFFERENT FROM B2 ($p < 0.05$).	50
TABLE 9. POLYNOMIAL TREND COMPONENTS BETWEEN NORMO- AND HYPER-THERMIC ASSESSMENT. DURING NORMOTHERMIA, THE VARIANCE OF THE TREND COMPONENTS EXPLAINING \bar{T}_{EXP} WAS SIMILAR TO THE VARIANCE TREND COMPONENTS OF CVC_{EXP} . HOWEVER, DURING HYPERTHERMIA, THE VARIANCE EXPLAINING CVC_{EXP} WAS NOT SIMILAR TO ANY OTHER TREND COMPONENT SPECIFICALLY.....	51
TABLE 10. SPECTRAL ANALYSIS OF THE CONTROL ARM DURING NORMO- AND HYPER-THERMIC ASSESSMENT. DATA ARE PRESENTED AS MEAN \pm S.E.M. ^A ENDOTHELIAL BAND DIVIDED INTO TWO SUBSECTIONS. ^B SIGNIFICANTLY DIFFERENT FROM NORMOTHERMIA ($p < 0.050$).	53
TABLE 11. SPECTRAL ANALYSIS OF THE EXPERIMENTAL ARM DURING EACH TEMPERATURE MANIPULATION DURING NORMO- AND HYPER-THERMIC ASSESSMENT. DATA ARE PRESENTED AS MEAN \pm S.E.M. ^A SIGNIFICANTLY DIFFERENT FROM A1 ($p <$ 0.050). ^B SIGNIFICANTLY GREATER FROM B1 ($p < 0.050$). ^C SIGNIFICANTLY DIFFERENT FROM NORMOTHERMIA ($p <$ 0.050).....	54

LIST OF FIGURES

FIGURE 1. BIPHASIC RESPONSE TO LOCAL HEATING (ADAPTED FROM (58)).	4
FIGURE 2. A REPRESENTATION OF A MICRODIALYSIS FIBRE. DRUGS ARE TYPICALLY DISSOLVED IN LACTATED RINGER'S SOLUTIONS AND CIRCULATED THROUGH THE FIBRE (69).	8
FIGURE 3. ROLE OF NITRIC OXIDE DURING PROLONGED LOCAL HEATING. THE TOP PANEL (A) SHOWS L-NAME INFUSED ~45 MIN INTO LOCAL HEATING. THE BOTTOM PANEL (B) SHOWS L-NAME INFUSION 45 MIN PRIOR TO AND DURING LOCAL HEATING (81).	14
FIGURE 4. REPRESENTATIVE TRACING FROM NON-SELECTIVE NOS AND EDHF INHIBITION IN RESPONSE TO LOCAL HEATING TO 44°C. EDHF INHIBITION AFFECTED NADIR AND THE PLATEAU. THE COMBINATION OF EDHF AND NOS INHIBITION ALLOWED FOR A SLIGHT INITIAL PEAK AND ALMOST INHIBITED THE PLATEAU IN RESPONSE TO LOCAL HEATING (8).	16
FIGURE 5. EFFECT OF BOTULINUM TOXIN INJECTION ON VASOCONSTRICTION (COLD STRESS), REFLEXIVE VASODILATION (WHOLE-BODY HEATING) AND LOCAL VASODILATION (LOCAL HEATING) RESPONSE COMPARED TO CONTROL (70).	19
FIGURE 6. VASODILATION ASSOCIATED WITH WHOLE-BODY HEATING DURING NOS (L-NAME), CYCLOOXYGENASE-1 AND -2 (KETO), AND NO (CONTROL) INHIBITION (79).	21
FIGURE 7. REDISTRIBUTION OF BLOOD IN A COOL AND HEAT STRESSED INDIVIDUAL. THE DARK AREAS REPRESENT HIGH AMOUNTS OF BLOOD VOLUME (ADAPTED FROM (90)). NOTE THE INCREASED SHADED AREAS REPRESENTING MORE BLOOD FLOW AT THE EXTREMITIES WHEN THE BODY IS HOT.	28
FIGURE 8. THE LEFT PANEL IS THE FOREARM INSTRUMENTED. I IS THE LASER-DOPPLER PROBE, II-IV ARE PROXIMAL (II), MIDDLE (III), AND DISTAL (IV) THERMOCOUPLES USED TO CALCULATE MEAN FOREARM TEMPERATURE. THE RIGHT PANEL IS THE FOREARM SUBMERGED AND POSITIONED FOR THE DURATION OF THE EXPERIMENT.	35
FIGURE 9. POSITIONING OF PARTICIPANT FOR THE DURATION OF THE EXPERIMENT.	37
FIGURE 10. REPRESENTATIVE DATA FROM ONE PARTICIPANT. THE TOP PANEL IS THE SKIN BLOOD FLOW RESPONSES, IN CUTANEOUS VASCULAR CONDUCTANCE AS A PERCENTAGE OF MAX, OF THE CONTROL (FILLED CIRCLES; CVC_{CON}) AND EXPERIMENTAL (OPEN CIRCLES; CVC_{EXP}) ARMS. 'A1' AND 'A2' REPRESENT THE NEUTRAL (33°C) EXPERIMENTAL ARM TEMPERATURE (\bar{T}_{EXP}) MANIPULATIONS, AND 'B1' AND 'B2' REPRESENT THE HOT (38.5°C) \bar{T}_{EXP} MANIPULATION. THE BOTTOM PANEL HAS \bar{T}_{EXP} (OPEN CIRCLES), CONTROL (FILLED CIRCLES; \bar{T}_{CON}), MEAN SKIN (OPEN UPWARD TRIANGLES; \bar{T}_{SK}), AND CORE (FILLED DOWNWARD TRIANGLES; T_{RE}) TEMPERATURE RESPONSES TO LOCAL AND WHOLE-BODY TEMPERATURE MANIPULATIONS.	45
FIGURE 11. CHANGES TO CVC (A) AND LDF (B) FROM T_{LOC} MANIPULATIONS DURING NORMO- (FILLED CIRCLES) AND HYPERTHERMIA (OPEN CIRCLES). *SIGNIFICANTLY DIFFERENT FROM HYPERTHERMIC MEASURES ($P < 0.05$). [^] SIGNIFICANTLY DIFFERENT FROM A1-B1 ($P < 0.05$). ^{^b} SIGNIFICANTLY DIFFERENT FROM B1-A2 ($P < 0.05$). ^{^c} SIGNIFICANTLY DIFFERENT FROM A2-B2 ($P < 0.05$).	48

LIST OF ABBREVIATIONS

Analysis of Variance	ANOVA
Blood pressure	BP
Bretylium tosylate	BT
Cold induced vasodilation	CIVD
Core temperature	T_c
Cutaneous vascular conductance	CVC
Endothelial dependent hyperpolarizing factors	EDHFs
Endothelial nitric oxide synthase	eNOS
Eutectic mixture of local anesthetics	EMLA
Heart rate	HR
Ketolorac	KETO
Liquid condition garment	LCG
Laser-Doppler flowmetry	LDF
Local temperature	T_{loc}
Mean arterial pressure	MAP
<i>N</i> ² -(diphenylacetyl)- <i>N</i> -([4-hydroxyphenyl]methyl)- <i>D</i> -arginine amide	BIBP-3226
Neuropeptide Y	NPY
Nitric Oxide	NO
Nitric oxide synthase	NOS
Neuronal nitric oxide synthase	nNOS
<i>N</i> ^G -nitro- <i>L</i> -arginine methyl ester	L-NAME
Norepinephrine	NE
<i>N</i> ^ω -amino- <i>L</i> -arginine	LNAA
<i>N</i> ^ω -propyl- <i>L</i> -arginine	NPLA
Propranolol	PRO
Rectal temperature	T_{re}

Skin blood flow	SkBF
Skin temperature	\bar{T}_{sk}
Sodium nitroprusside	SNP
Transient receptor potential vanilloid	TRPV
Yohimbine	YOH

CHAPTER ONE: INTRODUCTION

Changes in skin blood flow (SkBF) are one of the primary thermoregulatory responses in humans. The cutaneous vasculature responds in a strong and dynamic fashion depending on the environmental conditions, which can range from negligible flow values when exposed to cold stress, to up to $8 \text{ L}\cdot\text{min}^{-1}$ during heat stress (59, 90, 91). Changes in cutaneous circulation in nonglabrous (hairy) skin are mediated via two branches of the sympathetic nervous system (noradrenergic vasoconstrictor system and cholinergic vasodilator system), and a combination of local factors (12, 58, 59, 63). Research describing the responses of SkBF to thermal stress has been well documented (see Johnson et al., (59) for a comprehensive review), with core body temperature (T_c ; (12, 63)), mean skin temperature (\bar{T}_{sk} ; (59)), and local skin temperature (T_{loc} ; (8, 45, 58)) being important afferents.

Previous work has mainly focused on these thermal afferents individually (8, 26, 42, 45, 64, 81, 114), and a few have attempted to isolate them (9, 29, 57, 86, 97). Prior work has been limited by the ability to control different afferents simultaneously, without using techniques that modify SkBF control. Indeed, studies aiming to separate the roles of reflexive and local SkBF control have either used exercise (86), which leads to an elevated internal (core) temperature threshold for the onset of vasodilation (60, 67), studied glabrous (non-hairy) skin (9, 24, 29, 33), did not maintain thermoneutrality in the limb (33, 97), or did not manipulate T_{loc} during distinct T_c phases to observe the interaction of the two control mechanisms (57). If thermoneutrality is not maintained, the thermal background may evoke local control mechanisms such as endothelial nitric oxide synthase (eNOS; (71)), norepinephrine (NE; (49)), neuropeptide-Y (NPY; (46)),

endothelial dependent hyperpolarizing factors (EDHFs; (8)) or a host of other local factors (59). Not controlling T_{loc} during heat stress allows for reflexive vasodilation to increase T_{loc} . Due to logistical issues controlling temperature, little work (29, 33, 57, 97, 105) has been able to successfully isolate and quantify the relative contribution of peripheral (T_{loc}) or central (T_c) afferents regulating SkBF, while maintaining consistent thermal backgrounds.

Research designs have successfully isolated T_c and T_{loc} while focusing on other physiological variables such as neuromuscular function (109), finger cold-induced vasodilation (CIVD) (24, 29), and metabolic heat production and circulating catecholamines (33). Thomas et al. (109) were able to increase T_c by $\sim 2^\circ\text{C}$ while clamping muscle and skin temperature of one leg at thermoneutral through ice packs, successfully isolating central and peripheral afferents governing neuromuscular function (109). The studies attempting to isolate SkBF afferents (9, 24, 29, 33, 57) suggest that the central afferents play a dominant role in regulating physiological variables more than peripheral afferents. Importantly, when thermoneutrality is maintained in one arm and T_{loc} is increased to 42.5°C in the other, passively heating participants caused equal cutaneous vasodilation to occur, indicating that central afferents have a predominant role during hyperthermia (57). Overall, however, the relative importance of local control of SkBF during thermal stress remains unclear.

Therefore, the objective of this experiment was to isolate the roles of rectal temperature (T_{re}) and T_{loc} on forearm SkBF. This was achieved during both normo- and hyper-thermia ($\Delta T_{re} + 1.1^\circ\text{C}$) by alternating between a neutral (33.0°C) and hot (38.5°C) arm T_{loc} , while maintaining the other arm at thermoneutral (33.0°C). It is hypothesized

that: 1) T_{loc} will be the driving force behind cutaneous blood flow during normothermia, and 2) T_{re} will be the driving force for forearm SkBF during hyperthermia; SkBF will not respond to changes in T_{loc} .

CHAPTER TWO: LITERATURE REVIEW

Alterations in SkBF are one of the primary thermoregulatory responses in humans (58, 59). SkBF responds in a strong and dynamic fashion depending on environmental conditions, ranging from almost zero when exposed to cold stress to $8 \text{ L}\cdot\text{min}^{-1}$ in cases of heat stress (90, 91, 105). Two branches of the sympathetic nervous system, an adrenergic vasoconstrictor and a nonadrenergic vasodilator branch control cutaneous circulation (12, 43, 59). When a cold stimulus is applied to the skin, a decrease in blood flow termed reflexive vasoconstriction (59, 97) occurs in an attempt to maintain T_c at approximately 37.0°C . If the cold stress is intense and long enough, SkBF will be reduced to almost zero in an attempt to minimize heat loss (59, 90, 91). During heat stress SkBF increases in an attempt to dissipate heat through convective heat loss (14, 111). There is a bi-phasic vasodilation response to local heating (see Fig. 1 below) that consists of an initial peak followed by a brief portion of nadir, then a sustained plateau before it dies away (3, 58, 59).

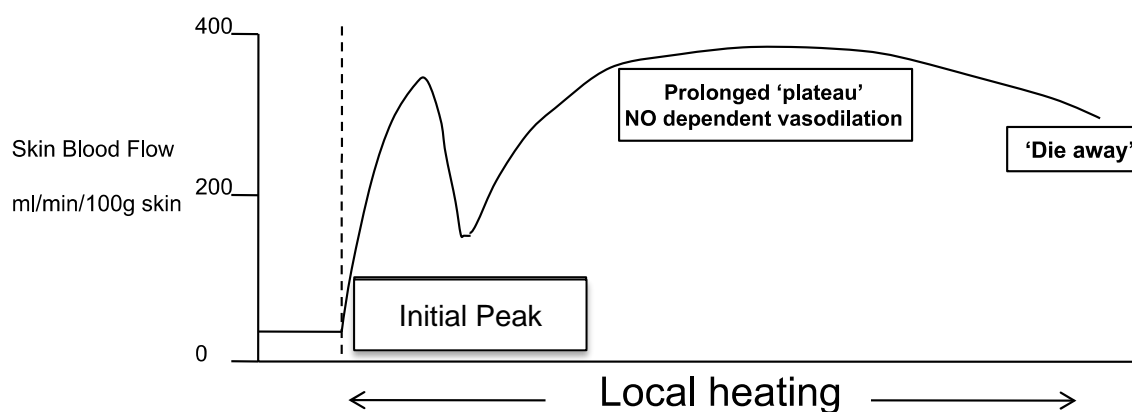


Figure 1. Biphasic response to local heating (Adapted from (58)).

Aside from thermoregulation, SkBF plays an integral role in blood pressure (BP) regulation through arterial baroreceptors (12, 21, 56, 62). Decreases in central blood volume occur during heat stress as the cutaneous circulation can receive as much as 60% of cardiac output (56, 90, 91). When baroreceptors detect that there is low central blood volume, peripheral vasoconstriction occurs in causing a redistribution of blood towards the brain, splanchnic and thoracic regions (12, 22). Activation of baroreceptors can occur due to changes in posture (upright *vs.* supine), which leads to peripheral vasoconstriction in both normo- and hyper-thermic conditions (12, 57, 62). Thermoregulatory and BP inputs can thus compete against each other to maintain T_c and central blood volume (21, 56). This review will discuss the mechanisms involved in three sections of local and whole-body heating, as well as the relationship between core and peripheral skin temperature, the mechanisms involved, and how thermal homeostasis is maintained.

2.1 Drugs used for Assessment of Skin Blood Flow

This review will begin with a survey of common drugs that have been extensively used in SkBF literature to study the mechanisms controlling cutaneous circulation and its response to local and/or whole-body heating, as well as their two major delivery methods. These drugs have high specificity, enabling certain aspects of cutaneous circulation to be studied by abolishing, inhibiting or antagonizing different pathways (See Table 1 for a list of commonly used drugs to studying mechanisms of SkBF). For example, bretylium tosylate (BT) is taken up by sympathetic nerve endings, which inhibits the reuptake and further release of NE and other neurotransmitters, thus, abolishing sympathetic contribution to cutaneous circulation (38, 68). To assess sympathetic contribution of SkBF, BT is applied to an experimental site while a control site is left untreated, or

‘treated’ with the delivery vehicle to ensure that its effect on SkBF is taken into account.

The difference in SkBF between the experimental and the control site allows for the contribution of the NE and co-neurotransmitters to be assessed (68).

Table 1. Common drugs used in skin blood flow work.

Name (Abbreviation)	Effect	Mechanism
Botulinum Toxin	Abolish cholinergic nerve activity	Presynaptically abolishes the release of acetylcholine and cotransmitters from cholinergic nerves (70)
Bretylium tosylate (BT)	Abolish sympathetic nerve activity	Presynaptically blocks the release of NE and cotransmitters from the sympathetic nerves (38)
<i>N</i> ² -(diphenylacetyl)- <i>N</i> -([4-hydroxyphenyl]methyl)- <i>D</i> -arginine amide (BIBP-3226)	Prevents NPY from binding to Y ₁ receptor. Acts in part to abolish sympathetic vasoconstrictor response	Postsynaptic blockade of NPY at Y ₁ receptors (46)
Nitro- <i>L</i> -arginine methyl ester (L-NAME)	Inhibits the production of NO	Non-selective NOS inhibitor (69)
<i>N</i> ^o -amino- <i>L</i> -arginine (LNAA)	Inhibits production of NO resulting from the eNOS isoform	Selective eNOS inhibition (71)
<i>N</i> ^o -propyl- <i>L</i> -arginine (NPLA)	Inhibits production of NO resulting from the nNOS isoform	Selective nNOS inhibition (73)
Propranolol (PRO)	Prevents NE from binding to β adrenergic receptors. Acts in part to abolish sympathetic vasoconstrictor response	Postsynaptic blockage of β adrenergic receptors (46)
Sodium nitroprusside (SNP)	Elicits a maximal vasodilation response	Nitric oxide donor (34)
Topical anesthetic (EMLA)	Sensory nerve blockade	Inhibits nerve impulses by blocking sodium channels (81)
Yohimbine (YOH)	Prevents NE from binding to α adrenergic receptors. Acts in part to abolish sympathetic vasoconstrictor response	Postsynaptic blockade of α adrenergic receptors (46)

2.2 Methods to Introduce Drugs into Skin Microvasculature

Microdialysis and iontophoresis are the two primary methods used to introduce pharmacological agents into the cutaneous circulation. These methods of introducing agents into the area do not have systemic effects and are highly localized. Other modalities to introduce drugs into the cutaneous vasculature are through a topical cream (i.e., EMLA) or injection (i.e., botulinum toxin).

2.2.1 Microdialysis

Microdialysis comprises of inserting a microdialysis fibre into the dermal layer of the skin, allowing for mechanistic investigations of the cutaneous circulation *in vivo* (2, 40). Typically ice or a local anaesthetic is applied to temporarily anaesthetise the skin before inserting the fibres. If ice or a local anaesthetic is not applied prior to inserting microdialysis fibres, peak cutaneous vascular conductance (CVC) response is attenuated (40). A 25-gauge needle is inserted into the dermal layer of the skin for approximately 2.5 – 3.0 cm. The microdialysis fibre is then fed through the lumen of the needle and the needle is then removed from the skin leaving the microdialysis fibre in place (2, 40, 49, 69). This protocol must be done 90 min before the experiment takes place to allow for the trauma to subside from inserting the fibres (2, 40).

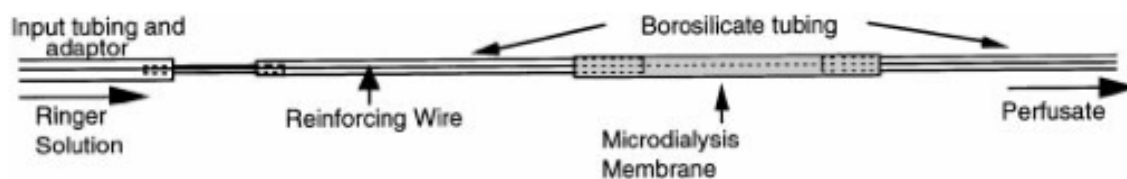


Figure 2. A representation of a microdialysis fibre. Drugs are typically dissolved in lactated Ringer's solutions and circulated through the fibre (69).

An advantage of microdialysis is that researchers are able to perform multiple interventions simultaneously due to the drugs' highly localized effects, and it is common to have four fibres on one forearm spaced 3 – 5 cm apart during an experiment (40). This is advantageous as it is time and cost effective, participants serve as their own control, and eliminates day-to-day variability. Drugs must be dissolved in an electrolyte (Ringer's) solvent in order to facilitate transportation in the microdialysis fibre as well as achieve the correct drug concentration. Ringer's solution serves as the control as it allows researchers to compare the direct effect of the drugs compared to the vehicle, which has been demonstrated to elicit no effect on SkBF (69). Drugs perfuse out of the fibre following their concentration gradients and into the skin at the semi-permeable membrane of the microdialysis fibre (69). Since microdialysis uses the drugs' concentrations to deliver it to the skin, larger and non-polar molecules can be delivered this way (which is an advantage over iontophoresis, discussed below). Intriguingly, an unexplored avenue is analysis on the subsequent neuropeptides that are in the perfusate due to their concentration gradient. Neuropeptides will move from areas of high concentration (tissue) to low concentration (microdialysis fibre), which then can be collected for subsequent analysis.

When employing microdialysis, several significant limitations or considerations exist. The first most obvious disadvantage is that the needle insertion to the skin that can cause trauma to the dermal layer and lead to inflammation (2, 40). In support of this, peak CVC during whole-body heating is significantly lower when the fibre is inserted without temporarily anaesthetising the skin with ice or a local anaesthetic (40). Second, the internal temperature when vasodilation begins is significantly higher when using

microdialysis (40), so care is needed in comparing microdialysis data to those using other SkBF manipulation techniques.

2.2.2 Iontophoresis

Iontophoresis is a non-invasive technique to apply chemicals to the cutaneous circulation in a highly localized manner. This method uses the electrical potential difference between the charge of the drug and the anode or cathode (depending on the polarity of the drug) of the iontophoresis system. An iontophoresis system uses a chamber to house the drug, laser-Doppler probe centered in the chamber, an electrode to supply the charge, and an optional temperature control unit. The electrode orientation depends on the polarity of the drug. The electrode matching the charge of the drug is attached to the iontophoresis chamber and the other is attached to the skin to create a ground. For example, the negative charge from the cathode and a negative charge from a drug (sodium nitroprusside) repel each other, and perfuse the drug through the dermal layer (85, 106). The chemical must be diluted in a non-conducting solvent so that the amount administered is directly proportional to the amount and duration of current applied (68, 85, 106).

Iontophoresis has no systemic effect and only affects a localized area ($< 1 \text{ cm}^2$) allowing for multiple experiments to be performed simultaneously (59). Iontophoresis is limited to drug molecules that are polar and that are sufficiently small to perfuse through the dermis. Further considerations that have to be accounted for with iontophoresis are that if the drug is diluted in an electrolyte solution (Ringer solution), both the drug and the electrolyte ions will be perfused into the dermis. When employing this method of drug delivery, the amount of drug perfused into the skin varies greatly from person to

person as skin conductivity can change (59, 106). Further considerations with iontophoresis are the length of experiments as the drugs are applied over a short time period (10 – 300 s) but have an ~80 min wash-in period for the effects of the drug to take place and for the current-induced hyperemia to subside (104).

2.3 Skin Blood Flow Response to Local Heating

The SkBF response to local heating has been well studied (43, 58, 59) over the past few decades. This response can be broken down into three sections (see Fig. 1): the initial peak, which is characterized by the initial rapid increase in SkBF, the plateau, which is the sustained vasodilation response to local heating, and the die away, which is a decrease in SkBF following extended periods of time of local heating (3, 58, 59).

2.3.1 Initial Peak

The initial response to local heating is characterized by a pronounced and rapid increase in SkBF in response to local heating. Full expression of the initial peak requires local vasodilators such as nitric oxide (NO) (71, 81), sensory nerves (11, 42, 81, 108), and intact sympathetic vasoconstrictor nerves (46, 48, 49).

NO is produced by nitric oxide synthase (NOS) during the conversion of L-Arginine to L-Citrulline (20). NOS is inhibited by the non-selective NOS inhibitor, nitro-L-arginine methyl ester (L-NAME) (69). NOS inhibition prior to rapid ($+0.5^{\circ}\text{C}\cdot 5\text{ s}^{-1}$) local heating significantly attenuated the increase in CVC compared to a group with functioning NOS by ~17% (81). During NOS inhibition with slow ($+0.1^{\circ}\text{C}\cdot 60\text{ s}^{-1}$) local heating, the initial peak is shifted to a higher temperature or completely abolished (49). These studies suggest that NO is required for full expression of the initial peak; however,

it may not be the most important pathway involved in the initial peak, as it is often only left shifted to a higher temperature threshold.

Sensory nerves play a large role in the initial response to local heating (11, 81, 107). During sensory nerve blockade with a topical anaesthetic (eutectic mixture of local anaesthetics; EMLA), the initial peak was reduced in magnitude (11, 42, 81, 108) as well as shifted to a higher temperature. Transient receptor potential vanilloid (TRPV) channels are activated by heat (98) and are located at the ends of cutaneous sensory nerves (115). Inhibiting TRPV-1 receptors with capsaizepine inhibited the initial peak by ~50%, whereas NOS inhibition only attenuated the initial peak by ~35% (115).

Sympathetic nerve function is presynaptically abolished with BT, which blocks the release of NE and other co-transmitters from sympathetic nerve endings (38, 68). Previously, it was thought that sympathetic nerves were only involved with cutaneous vasoconstriction, however, it has since been demonstrated that these nerves are required for full expression of vasodilation (45, 46, 49). Houghton et al. (49) were the first to investigate the role sympathetic nerves played in cutaneous vasodilation and established that the initial peak was abolished in response to local heating (46). However, the use of BT does not allow the determination if NE or NPY or a combination of the two is responsible as BT inhibits the release of all neurotransmitters from sympathetic nerve endings (38). Postsynaptic sympathetic blockade of NE is achieved by blocking α and β adrenergic receptors through yohimbine (YOH) and propranolol (PRO), respectively, (46). NPY is co-released with NE from sympathetic nerve endings and can be inhibited by blocking the Y1 receptor with N2-(diphenylacetyl)-N-([4-hydroxyphenyl] methyl)-D-

arginine amide (BIBP-3226). Postsynaptic inhibition using YOH and PRO, or BIBP-3226 shifted the initial peak to a higher temperature or abolished it in response to slow local heating (46). During complete postsynaptic sympathetic blockade with YOH, PRO, and BIBP-3226 the initial peak was abolished signifying that NE and NPY play an active role for full expression of the initial responses to local heating (46).

Rate of local heating influences the response to local heating. During presynaptic sympathetic blockade, BT abolishes the initial peak during slow ($+0.1^{\circ}\text{C}\cdot\text{min}^{-1}$) local heating to 42°C . However, the initial peak was preserved with BT, albeit at a less magnitude, during rapid ($+2^{\circ}\text{C}\cdot\text{min}^{-1}$) local heating (45, 46). If local heating is performed at a rapid rate causing a noxious stimulus (i.e., Rapidly to 44°C), the bi-phasic response to local heating is abolished and SkBF proceeds to directly to maximum (11).

2.3.2 Prolonged Plateau

The later portion of the biphasic response to local heating is termed the prolonged plateau, which is characterized by the stable portion of the response following the initial peak and nadir. This plateau is primarily NO-dependent (17, 58, 59, 69, 81), but also requires intact sympathetic nerves for full expression (45, 46). Infusion of L-NAME prior to- or during-local heating (81) resulted in decreased (Fig. 3A) or attenuated (Fig. 3B) vasodilation in response to local heating to 42°C , respectively. Infusing L-NAME during local heating rapidly decreased CVC to only 30% greater than baseline (69, 81). Local heating to 39°C has been demonstrated to produce a plateau that is almost entirely NO-dependent (17). When L-NAME is infused prior to and throughout local heating, vasodilation is significantly attenuated (46, 69, 81). Since these studies, different isoforms of the NOS have become available to study independently (71-73).

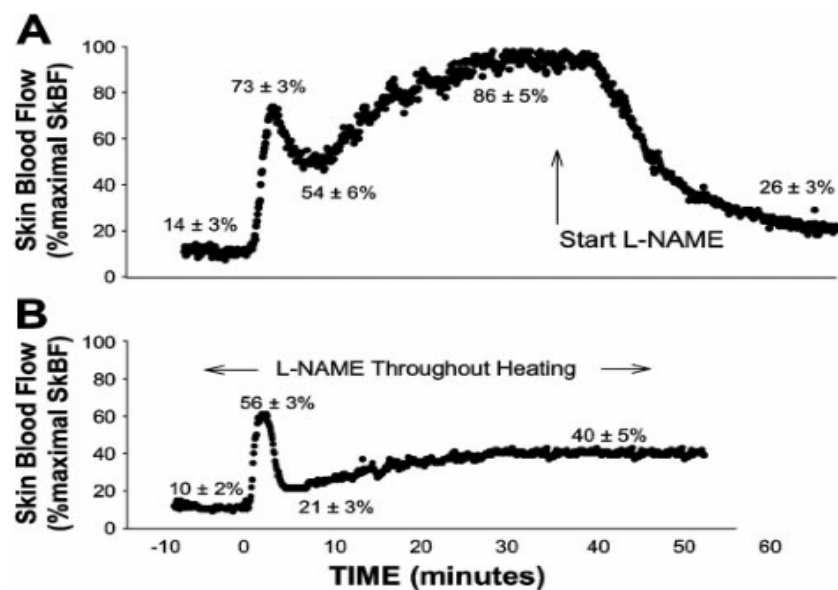


Figure 3. Role of nitric oxide during prolonged local heating. The top panel (A) shows L-Name infused ~45 min into local heating. The bottom panel (B) shows L-NAME infusion 45 min prior to and during local heating (81).

Of the three different isoforms of NOS, endothelial (eNOS) and neuronal (nNOS) have been demonstrated to be in high concentrations in human skin (7, 10). Inducible NOS is present in skin, albeit in small concentrations compared to e- and n-NOS and only reaches levels similar to the others following trauma and inflammation (7, 10). Endothelial NOS has been shown to play a critical role in vasodilation in response to local heating (71, 73). *N*^o-amino-L-arginine (LNAA) selectively antagonises the eNOS isoform while leaving other NOS isoforms intact (71). Local heating to 41.5°C under eNOS inhibition significantly attenuated the increase in CVC, whereas antagonism of nNOS had no effect on CVC (71, 73). Importantly, vasodilation occurs when NOS is inhibited, indicating mechanisms other than NO are at work.

Sensory nerves do not appear to play a role to the absolute magnitude of the plateau during local heating (11, 81, 108). TRPV-1 receptors are localized near sensory nerve endings and endothelial cells (115). TRPV-1 receptor inhibition with capsaizepine significantly attenuated plateau portion of the SkBF response to local heating (115).

EDHFs are a group of factors that are capable of causing cutaneous vasodilation by hyperpolarizing vascular smooth muscle through stimulating calcium-activating potassium channels (8, 59). EDHFs can be non-selectively inhibited via calcium-activating potassium channel antagonist tetrathylammonium, or certain factors can be selectively inhibited with other drugs. Tetrathylammonium reduces the plateau marginally from control, but when EDHFs and NOS are inhibited together, nearly all hyperemic response to local heating was abolished (Fig. 4, (8)). Exocyeicosatrienoic acid is a type of EDHFs that is selectively inhibited using a cytochrome P450 inhibitor, sulfaphenazole. Exocyeicosatrienoic acid inhibition during local heating slightly attenuates vasodilation demonstrating that they were responsible for about 50% of EDHF mediated vasodilation (8).

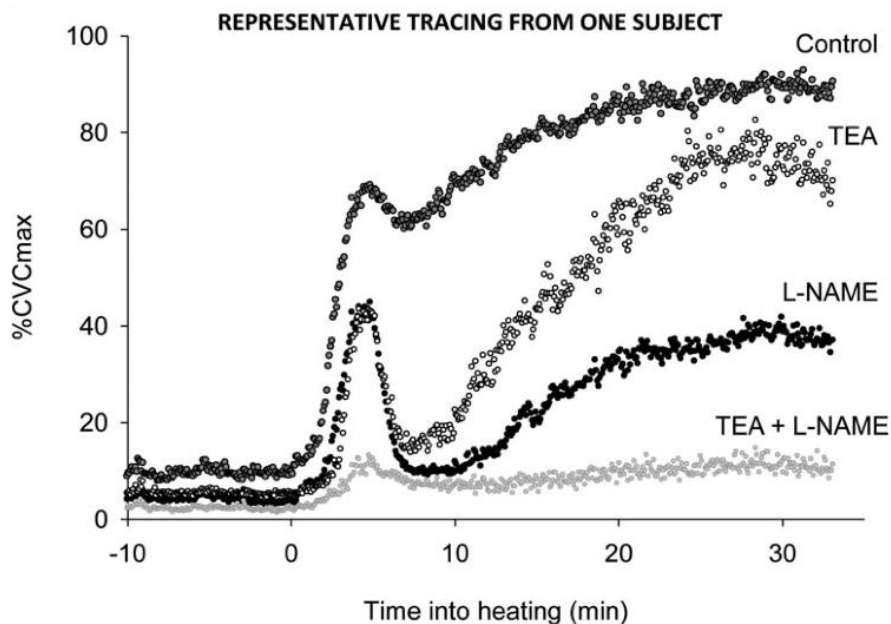


Figure 4. Representative tracing from non-selective NOS and EDHF inhibition in response to local heating to 44°C. EDHF inhibition affected nadir and the plateau. The combination of EDHF and NOS inhibition allowed for a slight initial peak and almost inhibited the plateau in response to local heating (8).

Similar to the initial peak, the plateau during prolonged heating requires intact sympathetic nerves for full vasodilation. Presynaptic blockade of sympathetic nerves with BT led to an attenuated prolonged vasodilation response during slow and rapid heating protocols (45). Postsynaptic blockade of either NE or NPY attenuated maximal SkBF response to local heating (46). When YOH, PRO and BIBP-3226 are administered at the same time there were no exacerbated effects on peak vasodilation, which supports the notion that these systems work in conjunction with each other as they are both released from sympathetic nerve endings (46).

2.3.3 Die Away

Following prolonged application of local heating to non-glabrous skin, a notable decrease in SkBF occurs (Fig. 1; (3, 45, 59)). Die away was initially observed by Barcroft and Edholm (3) using forearm submersion into water baths, and observed that it only occurs between 37 – 42.5°C. Recently, it has been found that this decrease in blood flow is sympathetically mediated (43, 45). Hodges et al. (45) found that when sympathetic function was presynaptically blocked with BT, the decreases in CVC did not occur.

2.4 Skin Blood Flow Response to Whole Body Heating

There are two primary methods researchers use to study the reflexive SkBF control, specifically an active and a passive model. Active models have participants exercise to induce an elevation in \bar{T}_{sk} , and if exercise is long and intense enough, an increase in T_c . Passive models involve participants either entering a water bath, warm air, or donning a liquid conditioning garment (LCG) to increase \bar{T}_{sk} and if the stimulus is applied for a prolonged period of time, an increased T_c . Two paths of heat loss occur, sudomotor activity (sweating) and cutaneous vasodilation. This section will focus on the reflexive cutaneous vasodilation response to whole-body heating.

2.4.1 Active Heating

During exercise, heat is generated internally by exercising muscles and a redistribution of blood occurs in an attempt to dissipate the heat produced (91). A competition for blood occurs with prolonged exercise as a result of the demand for blood to the working muscles, the cutaneous circulation to dissipate heat produced, and decreased plasma volume via sweating (36, 55). Blood is redistributed away from the splanchnic (91, 92) and cutaneous circulation (36, 55, 67) with the onset of exercise to

increase blood flow to areas of active skeletal muscle. An increase in sympathetic outflow at the onset of exercise is responsible for the vasoconstriction (67, 91, 92). Kellogg et al. (67) infused BT prior to exercise and abolished exercise induced cutaneous vasoconstriction.

During exercise, the T_c threshold that vasodilation occurs at is shifted to higher temperatures (55, 65-67, 74, 86). This shift is not due to sympathetic withdrawal, as inhibition of the sympathetic nervous system using BT did not have an effect on this temperature threshold (65-67, 86). The increase in T_c temperature threshold that vasodilation occurs at is increased following exercise (74) as well making thermoregulation increasingly difficult due to a reduction in convective heat loss abilities.

2.4.2 Passive Heating

A passive heating model involves creating a hot environment that heats the body from the outside. In response to a warm stimulus on the skin, there is increased blood flow to the cutaneous circulation, which heats the blood and returns it to the core heating both \bar{T}_{sk} and T_c in a feed-forward manner. More blood flow is sent to the cutaneous circulation as the body heats to attempt to limit heat gain, which facilitates increases to T_c . A popular method to induce passive heat stress is through the use of a LCG (34, 83, 109). These garments circulate hot water ($\sim 50^\circ\text{C}$) to raise \bar{T}_{sk} to $\sim 38.5^\circ\text{C}$ and T_c by a desired amount. Sympathetic withdrawal is responsible for the initial portion of vasodilation at rest (27, 32, 37, 86, 89). Pretreating areas with BT failed to initially increase SkBF in response to whole-body heating, whereas control sites did increase SkBF (65). Vasodilation due to sympathetic withdrawal is only responsible for 5 – 15% of vasodilation and the remaining 85 – 95% is due to active vasodilation (12, 22, 56).

Active vasodilation from passive heat stress is mediated through cholinergic nerves (59, 70, 100). Botulinum toxin A can be injected to presynaptically inhibit the release of acetylcholine and associated neurotransmitters to elucidate the role of cholinergic nerves involvement in active vasodilation (70). An intradermal injection of botulinum toxin abolished active vasodilation in response to whole-body heating (Fig. 5, (70)). Acetylcholine released from cholinergic nerves play an important role in the early response to heat stress as inhibition facilitated an earlier body temperature threshold for vasodilation to occur, however, it did not have an effect once SkBF began to notably increase (100).

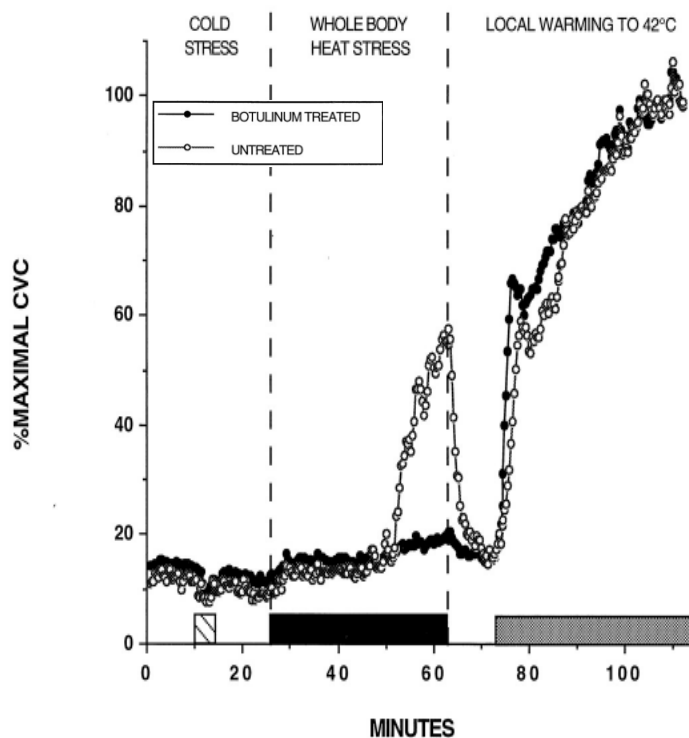


Figure 5. Effect of botulinum toxin injection on vasoconstriction (cold stress), reflexive vasodilation (whole-body heating) and local vasodilation (local heating) response compared to control (70).

Nitric oxide plays an important role facilitating vasodilation in response to whole-body heating (64, 72, 73, 81, 99). NOS inhibition during passive heat stress between 0.6 – 1.0°C significantly attenuated the SkBF response compared to control (64). Infusing 7-nitroindazole (72) or *N*^ω-propyl-L-arginine (NPLA) (73) selectively inhibits the nNOS isoform allowing for its contribution to reflexive vasodilation to be assessed. Reflexive vasodilation was augmented during nNOS inhibition (72), but was not affected during eNOS inhibition (71, 73). NOS activity is required for full expression of vasodilation, as it is not completely abolished during NOS inhibition suggesting there are other mechanisms at play.

Sensory nerves have been exposed to play a role in the sensitivity of reflexive vasodilation, as EMLA application delayed the onset of it (113). Inhibition of sensory nerves alone do not affect CVC during passive heating, but when sensory nerve and NOS were inhibited, CVC was significantly lower than NOS inhibition alone (113). TPRV-1 receptors are responsible for a small portion of the sensitivity and absolute magnitude of the reflexive cutaneous vasodilation response (114).

Prostaglandins are involved in many physiological roles throughout the human body, one of which is to facilitate vasodilation. Cyclooxygenase-1 and -2 are important enzymes in the formation of prostanoids, which can be inhibited using ketolorac (KETO). The vasodilatory plateau reached during cyclooxygenase inhibition was attenuated compared to control (Fig 6. (79)). A further reduction in CVC occurred with combined inhibition of NOS and prostanoids suggests that these two pathways are independent of each other (79).

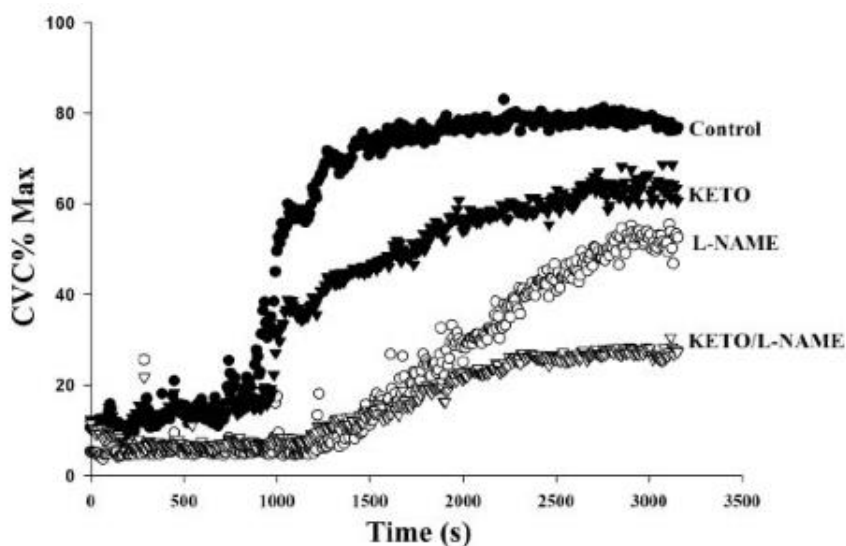


Figure 6. Vasodilation associated with whole-body heating during NOS (L-NAME), Cyclooxygenase-1 and -2 (KETO), and no (control) inhibition (79).

2.5 Methods to Measure Skin Blood Flow

2.5.1 Venous Occlusion Plethysmography

Venous occlusion plethysmography involves inflating a blood pressure cuff to less than arterial diastolic pressures but greater than venous pressure (59). Alternatively, a method is to inflate a distal cuff to suprasystolic pressures (i.e., 200 mm Hg) and a proximal occlusion cuff inflated to just under diastolic pressure to allow blood flow into the limb (19, 97). This allows blood to flow into the limb while trapping blood distal to the cuff; therefore the rate of volume increase of the limb directly proportional to the amount of blood flowing into it. A strain gauge is placed on the midpoint of the forearm which measures the amount of volume increase occurs during occlusion (97). An advantage of using plethysmography is that the values can be expressed as absolute flow value ($\text{ml} \cdot 100 \text{ g}^{-1}$) (59, 97).

Venous occlusion plethysmography is limited to limbs that are large enough for a blood pressure cuff and a strain gauge placed distal to the cuff. Areas that plethysmography can be used are the forearm, calf, hand, and foot (59). Plethysmography is not limited to the measurement of SkBF but also underlying muscle blood flow as the gauge measures changes in total limb volume (19, 57). Further difficulties with plethysmography are that during periods of rapid increases in SkBF, such as rapid whole-body- or local-heating or cooling, errors can occur when determining SkBF from total forearm blood flow (97). This is partly due to the measurement schedule of plethysmography only allowing for two to four times per minute, and is therefore unable to capture rapid changes to cutaneous circulation (105). Since plethysmography is not a continuous digital signal, further analysis of the signal is not possible using this method.

2.5.2 Laser-Doppler Flowmetry

Laser-Doppler flowmetry (LDF) involves emitting laser light into tissue delivered from a fibre optic probe. Light is then scattered into the tissue being studied and partly absorbed. A LDF probe is primarily composed of a sender and a receiver. The sender delivers the laser light into the skin and the receiver picks up light that is reflected back. The beam of light being emitted from the sender has a wavelength of 780 nm. If the light comes in contact with a static object (i.e., arterial wall), the light being returned to the receiver will be the same wavelength as it was from the sender. When light hits a moving object (i.e., red blood cell) it undergoes a Doppler shift (change in wavelength) (87) before being picked up by the receiver. The amount of Doppler shift that the light undergoes depends on the number of cells and the velocity of the cells that the light makes contact with (87). The Doppler shifted light is returned to the receiver, converted

into an electrical signal, and returned as arbitrary ‘perfusion units’. Importantly, perfusion units are related to red blood cell flux, and not flow, as vessel diameter is not attainable with LDF measurements. Red blood cell flux is the product of the concentration of moving blood cells and their respective velocity.

Criticisms of LDF measurements are that there is a lack of consistency for the depth of measurement and its inability to measure blood flow (87). Depth of measurement depends on many factors including the concentration of capillaries, pigmentation of skin, oxygenation of blood, etc. However, the depth of measurement on the skin is approximately 0.5 – 1.0 mm, whereas when measuring other tissue such as the liver or the spleen, which have a much higher density of cells than skin, will have a much smaller depth of measurement. Measurement depth of 0.5 – 1.0 mm is due to the separation of probes being 0.25 mm, and a wavelength of 780 nm (87). Regardless of the fact there is no true depth measurement, Saumet et al. (96) demonstrated that LDF is not affected by underlying muscle blood flow during exercise and is an accurate representation of SkBF. Since red blood cell flux and not flow is reported using LDF, data is commonly normalized to maximal values by heating the site of measurement to 44°C and maintained until values stabilize (42, 108, 110).

There are many advantages to using LDF to assess SkBF. It is capable of capturing real time changes to the skin microvascular circulation. This is advantageous over plesytmography because LDF is able to capture abrupt changes to SkBF following temperature or drug manipulations. Another advantage of LDF is the non-invasive nature of the technique, whereas former methods involved injecting radioactive substances (xenon, radioactive microspheres) into the circulation (87), or having participants wear

multiple blood pressure cuffs and strain gauges. Its versatility compared to plethysmography is advantageous as laser-Doppler probes can be placed almost anywhere, from the fingertips (30) to the forehead (4), and investigate differences between glabrous and nonglabrous skin. This is beneficial when assessing SkBF during cold exposure to the extremities, and also looking at clinical populations and the effect of the disease on SkBF and to see if they are at an increased risk of circulatory diseases. Perhaps one of the strongest advantages of LDF is that the signal can be decomposed and allows insight into the mechanisms influencing SkBF without introducing drugs or needles into the cutaneous circulation.

2.4.2.1 Wavelet Analysis

Wavelet analysis involves decomposing the LDF signal into frequency and time components, offering high resolution for both. Unlike sinusoids involved with the fast Fourier Transform, wavelet transforms have discrete beginnings and endings that are translocated along the signal allowing for both high time and frequency resolution (1, 6, 50, 51, 103) High frequencies take a very short period of time to complete their period and allow for good time and frequency resolution, however, low frequency components take longer to complete their period, requiring longer time windows that create poor time resolution. Wavelet analysis has been shown to demonstrate accurate time and frequency resolution at both low and high frequencies (1, 6, 50, 51, 103).

The fast Fourier Transform involves using sinusoids infinitely long to recreate a signal that allows for high frequency resolution, however does not allow for detection of when an event occurred in time (35). The short-time Fourier Transform utilizes shorter time windows that allows for better time resolution, however does not facilitate good low

frequency resolution (102). The physiological control mechanisms of SkBF are composed of nonstationary components and are very low frequencies (as low as 0.005 Hz), which make the short-time- and the fast-Fourier Transform inadequate (6, 101, 103).

Signals can be reconstructed and analyzed using a combination of sine waves of varying frequencies and amplitudes. Decomposing the laser Doppler signal using wavelet analysis allows for the investigation of the physiological control mechanisms of SkBF. The frequency domain of interest for blood flow dynamics is between 0.005 – 2.0 Hz (6, 50, 51, 76, 103). The frequency of the heart rate is the upper frequency limit (2 Hz) as it is the fastest physiological rhythm associated with vasomotion (103). Vasomotion can be broken up into six frequency domains that correspond to physiological functions (6, 35, 75, 76, 103). The frequency band associated with endothelial function can be further broken down into a NO-independent and a NO-dependent frequency range (51, 75, 76). The highest peak frequency of around 1 Hz is associated with an individual's heart rate. This peak can change based on fitness level, with fit individuals demonstrating a peak close to 0.6 Hz, whereas the peak in individuals with a cardiovascular impairment was at 1.6 Hz (103). The peak around 0.27 Hz is related to respiratory activity. The peak around 0.10 Hz is related to myogenic activity, which is responsible for the oscillations observed in vasomotion and caused from changes in intra-arterial pressures (6). The peak around 0.04 Hz is related to neurogenic activity. The lowest peak around 0.01 Hz is associated with local metabolic activity, such as NO and prostaglandins (35).

Table 2. Frequency and their corresponding physiological function of vasomotion. ^aThe endothelial band broken up into an endothelial-independent and -dependent aspect (76).

Frequency Band (Hz)	Corresponding Physiological Function
0.0095 – 0.02	Endothelial
0.005 – 0.01	NO-independent ^a
0.01 – 0.02	NO-dependent ^a
0.02 – 0.05	Neurogenic
0.05 – 0.15	Myogenic
0.15 – 0.4	Respiratory
0.4 – 2.0	Cardiac

What makes wavelet analysis appealing is that much of the information that can be obtained was previously only available through pharmacological interventions. For example, in order to assess sympathetic activity with drugs, researchers would have to apply BT through iontophoresis (68) or microdialysis (44) to presynaptically abolish the sympathetic control of SkBF and compare the differences between treated and untreated sites. The difference between the treated and the untreated site would be attributed to sympathetic regulation of SkBF. Analyzing the frequency band associated with neurogenic activity can assess the sympathetic contribution to SkBF during thermal, orthostatic, exercise, etc., stress.

Although there are many different types of wavelets that can be used including the Daubechies, Haar, lognorm, and Morlet wavelet (1, 50, 51), the Morlet wavelet is the most popular choice when studying blood flow dynamics (6, 54, 103). The Morlet wavelet is a Gaussian (normal distribution) function that has been altered with a sine wave (6) and is used most commonly in blood flow dynamic research as it offers good time and frequency resolution following the uncertainty principal (6, 50, 51).

2.6 Thermal Balance

Alterations to SkBF are one of the human body's primary defence mechanisms against thermoregulatory challenges. Internal heat production comes from metabolic energy pathways and contracting muscles. External heat loss or gain is a result from convective, conductive, radiative and evaporative sources. Internal heat production and external heat loss or gain is depicted in the heat balance equation:

$$\dot{S} = \dot{M} \pm \dot{W} \pm \dot{R} \pm \dot{C} \pm \dot{K} - \dot{E}$$

\dot{S} is heat storage within the body. When this value is positive, it represents a gain in heat leading to hyperthermia. A negative value indicates a net heat loss by the body, which can lead to hypothermia. \dot{M} is metabolic heat production, \dot{W} is external work performed, \dot{R} , \dot{C} , \dot{K} , and \dot{E} are radiative, convective, conductive and evaporative heat losses or gains, respectively (14, 80).

In cold stress, thermal homeostasis is maintained by decreasing the amount of heat lost to the environment through evaporative, conductive and convective pathways through vasoconstriction and piloerection (111). In cases of heat stress, SkBF increases in an attempt to maintain thermal homeostasis by increasing the amount of heat dissipated to the environment by evaporative, conductive and convective heat loss (111).

A redistribution of blood occurs with heat stress (90, 91). Heat applied to the skin causes an increase in blood flow to the extremities in an attempt to decrease heat gain. With heat stress, cutaneous vasodilation occurs and there is an increased blood flow to the extremities (especially the hands and feet) to act as heat exchangers (9). The increase

in cutaneous blood flow is mediated by vasoconstriction and a decrease blood flow to the splanchnic region (Fig. 7, (91)).

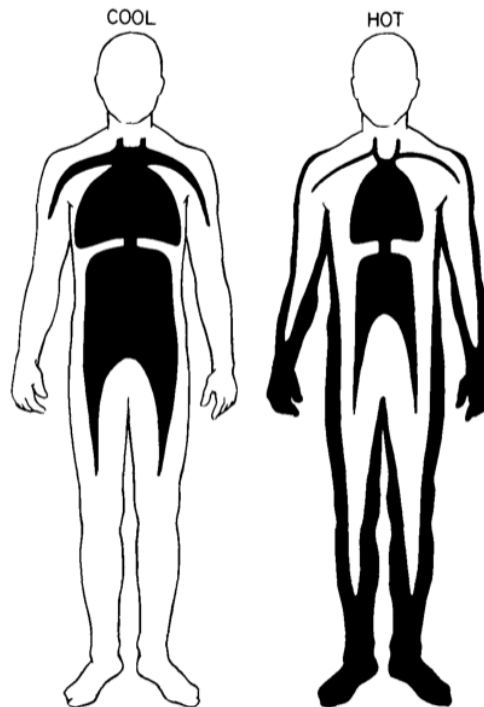


Figure 7. Redistribution of blood in a cool and heat stressed individual. The dark areas represent high amounts of blood volume (Adapted from (90)). Note the increased shaded areas representing more blood flow at the extremities when the body is hot.

2.6.1 Core Temperature

Previous work has largely investigated the mechanisms behind SkBF in response to local or whole body temperature manipulations (43, 58, 59), with changes to either \bar{T}_{sk} or T_c , yet only a few have successfully isolated the afferent inputs (33, 57, 97, 105, 116, 117). Previous work (57, 105, 116, 117) has shown that increasing local arm temperature surges SkBF during normothermia, and during passive heating reflexive vasodilation occurs in the control arm from whole-body heat stress even when it is maintained in a

thermoneutral background. They concluded that passive heat stress to $\Delta+1^{\circ}\text{C}$ above baseline temperature induced maximal vasodilation (105), and that reflexive control of SkBF is more influential than local control of SkBF (57, 116, 117). Importantly, no local temperature manipulations were performed during hyperthermia to determine if the interaction between local- and reflexive-control mechanisms of SkBF

Core temperature plays a large role in many physiological adaptations. Frank et al. (33) studied the isolated effects of skin temperature and core temperature on SkBF, metabolic heat production and circulating catecholamines by manipulating \bar{T}_{sk} via the use of two temperature controlled mattresses, and rapidly cooled T_c by 1.5°C by injecting a large quantity of 4°C saline. Through multiple regression analysis, it was determined that T_c influenced SkBF in glabrous skin was 3.1 times more than \bar{T}_{sk} increased metabolic heat production 2- and 3-fold for neutral (34°C) and cold (30°C) skin, respectively, and increased circulating epinephrine and NE 1.8 and 3.0 times more than \bar{T}_{sk} (33). Contrary to SkBF, CIVD research has had considerable attention in the past decade concerning the CIVD response in relationship to T_c and \bar{T}_{sk} (29-31). Importantly, CIVD occurs in areas of glabrous, non-hairy skin that is only innervated by sympathetic vasoconstrictor nerves, whereas sympathetic vasoconstrictor and cholinergic nerves (15, 23, 59) innervate SkBF in nonglabrous, hairy, skin. CIVD originates from arterio-venous anastomoses (AVAs) that are deep within the tissue and only regulated by sympathetic vasoconstrictor nerves (15, 23).

Core temperature plays a critical role for CIVD occurrences. After the initial decrease in \bar{T}_{sk} due to cold exposure, a CIVD occurrence is denoted by an increase in

finger temperature. There is discrepancy of a tangible definition of how much of an increase in finger temperature qualifies as a CIVD occurrence, however a range of $\Delta +0.5$ to $+4^{\circ}\text{C}$ is common throughout the literature (15, 16) measured by thermistors placed on the fingertip or toe. Previous work has shown that CIVD occurs more when body temperature is elevated (24, 29-31). CIVD events occurred most often when immersing the hand in cold water (24, 29), or being exposed to cold air (30, 31), and when T_c was above baseline. Recently it was shown that most CIVD events occur when mean body temperature (a combination of \bar{T}_{sk} and T_c) is above baseline levels (29-31). Utilizing an A-B-A-B (warm-cold-warm-cold) protocol, Flouris and Cheung (29) demonstrated that CIVD occurred when T_c was above baseline levels but body heat content was negative. However, when T_c fell below baseline, CIVD did not occur and blood flow to the finger was almost non-existent (29). During another A-B-A-B protocol, these authors concluded that finger blood flow was a function of the rate of change to mean body temperature and heat storage (30).

2.6.2 Skin Temperature

Humans have an innate ability to adapt behaviourally and physiologically. Behavioural adaptations appear to be driven equally by both \bar{T}_{sk} and T_c input (33), which plays an important role in human behavioural adaptation to alterations in temperature. This study demonstrated that physiological adaptations are largely related to T_c whereas behavioural changes are more equally dependent on T_c and \bar{T}_{sk} .

Skin temperature plays an important role in protecting T_c from external cold stimulus. Lowering whole body skin temperatures increase the internal temperature threshold for active vasodilation to occur (86), in order to maintain current T_c . Skin

temperature plays an important role in reflexive vasoconstriction in an attempt to maintain T_c . Savage and Brengelmann (97) rapidly reduced \bar{T}_{sk} by 2°C with one forearm exposed to temperature alterations, and one forearm bare to the surrounding room environment. Rapid reduction in mean body skin temperature of 2°C resulted in net vasoconstriction in both the exposed and non-exposed forearm in an attempt to limit convective heat loss (97) leading to an increase in T_c , suggesting that reflexive vasoconstriction was able to protect core body temperature.

2.6.3 Skin and Core Temperature Interaction

Physiological and behavioural adaptations that humans make are modulated by both central and peripheral inputs, however much of the previous literature has only studied the effects one of the other (46, 49, 58, 73). From these studies, many mechanisms controlling SkBF in response to local and whole body temperature manipulations (43, 58, 59), as well as exercise (55), are known. However, the isolation of \bar{T}_{sk} and T_c has not been well studied (57). Clearly, T_c does play a role in SkBF regulation as demonstrated by a collection of studies looking at thermal balance and CIVD occurrences (29-31), however it is still unclear whether T_c or local \bar{T}_{sk} is what regulates SkBF, and what are the mechanisms behind this.

CHAPTER THREE: OBJECTIVES AND HYPOTHESIS

3.1 Objectives

The objectives of this study are to:

1. Determine if T_{re} or T_{loc} is the driving force of forearm SkBF by comparing an arm maintained at thermoneutral (33°C) and the other's T_{loc} being manipulated in an A-B-A-B fashion between neutral (*A*; 33°C) and hot (*B*; 38.5°C) during normo- and hyper-thermia ($\Delta T_{re} + 1.1^{\circ}\text{C}$).
2. Perform spectral analysis on the laser-Doppler signal to determine the mechanisms behind SkBF control during normo- and hyper-thermia.

3.2 Hypotheses

The specific hypotheses of this study are:

1. T_{loc} will be the driving force behind forearm SkBF during normothermia.
2. Forearm SkBF will not respond to T_{loc} changes during hyperthermia.
3. Reflexive vasodilation during hyperthermia will increase skin blood flow to the control arm.

CHAPTER FOUR: METHODS

4.1 Sample Size Estimation and Participant Characteristics

The study was approved by the Bioscience Research Ethics Board of Brock University (BREB #13-283) and conformed to the standards set by the Declaration of Helsinki. All participants were informed of the experimental protocol and the associated risks prior to participating in the experiment. Verbal and written consent was obtained from each participant.

Cohen (18) says a ratio of 4:1 should be made between Type II and Type I error. Therefore, the ratio adopted for this study was 4:1 with $\beta = 0.20$ and $\alpha = .05$, resulting in a power $(1 - \beta)$ equal to 0.80. Pilot data and *a priori* power analysis demonstrated that 8 participants would be required for such a study.

To accommodate for potential participant dropout or technical issues, 10 healthy and active individuals (7 males and 3 females) were recruited for the experiment with no diagnosed metabolic or cardiovascular diseases; participants also did not smoke or take any prescribed medication other than oral contraceptives. In order to control for sex differences in thermoregulation, females were tested within the first 10 days of the onset of self-reported menses, or during the placebo/no pill phase if taking oral contraceptives, as no sex-related difference in maximal SkBF are observed during this phase from passive heating (34). The mean (\pm SD) for age, height, mass, body fat percentage, and peak oxygen uptake ($\dot{V}O_{2\text{peak}}$) of all participants was 23.1 ± 1.8 years, 173.3 ± 7.4 cm, 65.3 ± 7.9 kg, 13.8 ± 5.8 %, and 56.4 ± 5.2 ml·kg⁻¹·min⁻¹, respectively.

4.2 Experimental Design

All participants completed a familiarization and an experimental session. Participants were instructed to avoid strenuous exercise and caffeine 12 h prior, and alcohol consumption 24 h prior to the experimental session. Additionally, participants were advised to have a light meal 1 to 2 h before the experimental session, and instructed to drink water *ad libitum*. During the familiarization session, height, weight, body fat percentage (%), and $\dot{V}O_{2\text{peak}}$ were determined. Height and weight were measured with standard laboratory equipment. Body fat percentage was calculated through a 7-site skinfold measurement (52, 53) with manual calipers (Harpender, Bay International, West Sussex, UK). $\dot{V}O_{2\text{peak}}$ was determined through indirect calorimetry (Gas Analyzer, ADInstruments; Labview software) during a progressive running test until volitional exhaustion on a treadmill (Trackmaster TMX22, Full Vision Inc., Newton, KS, USA).

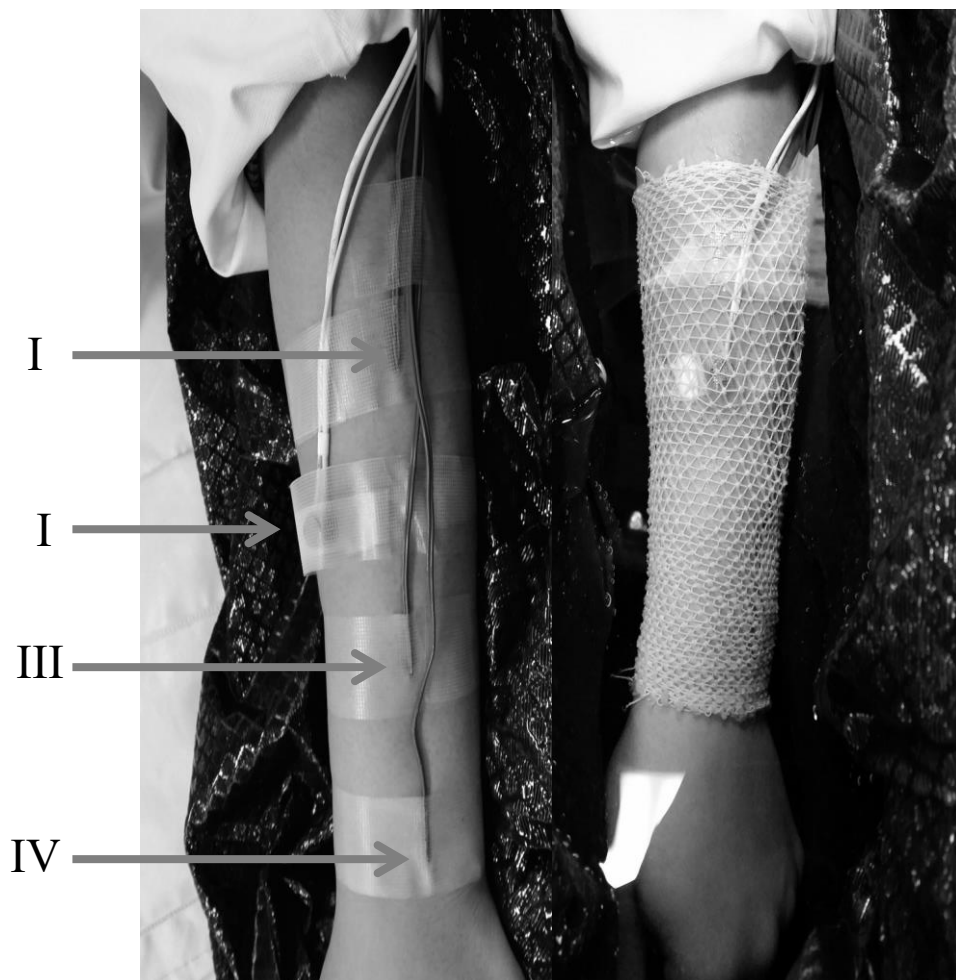


Figure 8. The left panel is the forearm instrumented. I is the laser-Doppler probe, II-IV are proximal (II), middle (III), and distal (IV) thermocouples used to calculate mean forearm temperature. The right panel is the forearm submerged and positioned for the duration of the experiment.

Participants arrived at the laboratory ($\sim 22^{\circ}\text{C}$, $\sim 35\%$ relative humidity) between 0800 – 1200 h for the experimental session. Euhydration was confirmed using a refractometer (PAL-10S, Atago, USA) and defined as a urine specific gravity (USG) ≤ 1.020 . If the participant was hypohydrated (USG > 1.020), 0.5 L of water was given and USG was reassessed after 30 min. If participants were still hypohydrated, testing was

rescheduled. If euhydration was confirmed, participants were instructed to self-insert a rectal thermistor (Mon-A-Therm Core, Mallinkrodt Medical, St. Louis, MO, USA) 15 cm beyond the anal sphincter to assess rectal temperature (T_{re}).

Thermocouples (PVC-T-24-190, Omega Environmental Inc., Laval, QC, CAN) were taped (TransporeTM, 3M, St. Paul, MIN, USA) to the chest, thigh, upper arm and calf to calculate mean skin temperature (\bar{T}_{sk}), calculated using the weighted average of the four thermocouples (88):

$$\bar{T}_{sk} = 0.3(\text{thigh}) + 0.3(\text{chest}) + 0.2(\text{calf}) + 0.2(\text{arm}).$$

Participants then dressed in a three-piece liquid conditioning garment (LCG; BCS 4 Cooling System, Allen Vanguard, Ottawa, ON, CAN), consisting of 1/8" diameter Tygon tubing sewn over stretchable hood, torso, arms, and legs; the face, forearms, hands, and feet were left uncovered. Males wore only shorts and females wore shorts and a sports bra under the LCG to expose a large amount of skin to facilitate heat transfer to the body. To eliminate evaporative heat loss, a polyvinyl rain suit was worn over the LCG. Water temperature of the LCG was manipulated by adding hot or cold water, maintained at a constant temperature by a temperature controller (Model 5202, Polyscience, Niles, IL, USA) and pumped (MED-ENG, Pembroke, CAN) at a flow rate of $\sim 1.5 \text{ L}\cdot\text{min}^{-1}$.



Figure 9. Positioning of participant for the duration of the experiment.

The dorsal surface of each forearm was equipped with three thermocouples (Omega Environmental Inc.) located on the proximal, middle, and distal portion to calculate mean forearm temperature (Fig. 8). Red blood cell flux was assessed with laser-Doppler flowmetry (5010 LDPM, Perimed, Järfälla, Sweden) and used to provide an index of SkBF (61, 96). A combined laser-Doppler flux (LDF) and skin heater probe (Probe 451, Perimed) was taped (PF 105-3, Perimed and Transpore™, 3M) to the dorsal surface of each forearm. Thermocouples and LDF probes were held in place with nylon wrapping (BurnNet, Glenwood Laboratories, Oakville, ON, CAN). Participants sat semi-

recumbent in a Kore-Kooler® Rehab Chair (DQE, Fishers, IN, USA) with feet elevated to the height of their pelvis (Fig. 9). Each hand and forearm was immersed in individually temperature controlled water baths (Glad ForceFlex® Contractor Bags, Clorox Company of Canada, Brampton, ON, CAN) insulated with solar blanket for the duration of the experiment. During the ‘B’ manipulations (see 4.3 Experimental Protocol), the experimental arm was kept warm with a heated blanket (Life Brand Heating Pad, Brampton, ON, CAN).

4.3 Experimental Protocol

See Figure 10 for a schematic of the protocol and Table 3 for temperatures attained during each block of the protocol. The protocol began by circulating water through the LCG to obtain a \bar{T}_{sk} of $\sim 33^{\circ}\text{C}$, and forearm baths were adjusted to make both forearm temperatures $\sim 33^{\circ}\text{C}$. Once LDF values were stable, 5 min of baseline (A1) data were collected. Control forearm temperature (\bar{T}_{con}) was maintained at $\sim 33^{\circ}\text{C}$ for the duration of the normo- and hyper-thermic assessment. Following A1 measurements, experimental forearm temperature (\bar{T}_{exp}) was rapidly increased to 38.5°C (B1) and maintained for 5 min. A second ‘A’ measurement occurred by returning \bar{T}_{exp} to 33°C (A2) for 5 min. The final ‘B’ measurement (B2) ensued by increasing \bar{T}_{exp} to 38.5°C for 5 min. Following the final ‘B’ measurement, participants were passively heated by increasing the water temperature circulating through the LCG from $\sim 32^{\circ}\text{C}$ to $\sim 49.5^{\circ}\text{C}$ to elicit a 1.1°C rise in T_{re} above baseline values (the temperature from the last 60 seconds of normothermic measurements).

Table 3. Rectal (T_{re}), skin (\bar{T}_{sk}), control (\bar{T}_{con}), and experimental (\bar{T}_{exp}) arm temperatures ($^{\circ}C$) during each manipulation. Each ‘A’ and ‘B’ manipulation was approximately 5 min. T_{re} displayed is hypothetical data as each participant began at different temperatures. The light grey area is when participants were passively heated to increase T_{re} , and the dark grey area is when local skin heating occurred at the site of blood flux measurements was performed to obtain maximal flux values.

	A1	B1	A2	B2		B1	A1	B2	A2	
\bar{T}_{con}	33	33	33	33	Whole Body Passive Heating	33	33	33	33	Local Heat to 44$^{\circ}C$
\bar{T}_{exp}	33	38.5	33	38.5		38.5	33	38.5	33	
\bar{T}_{sk}	33	33	33	33		38.5	38.5	38.5	38.5	
T_{re}	37.1	37.1	37.1	37.1		38.2	38.2	38.2	38.2	

After T_{re} increased $1.1^{\circ}C$, 5 min of hyperthermic baseline data collection was performed. Again, \bar{T}_{con} was maintained at $33^{\circ}C$ throughout and \bar{T}_{exp} was manipulated in 5 min blocks. Measurements began with \bar{T}_{exp} at $38.5^{\circ}C$ (B1) for 5 min before being decreased to $33^{\circ}C$ (A1). After 5 min, \bar{T}_{exp} was returned to $38.5^{\circ}C$ (B2). \bar{T}_{exp} was again decreased to $33^{\circ}C$ (A2) after 5 min. Following the fourth temperature manipulation, maximal CVC was attained by increasing both LDF probes’ temperature from $33^{\circ}C$ to $44^{\circ}C$, at a rate of $3^{\circ}C \cdot min^{-1}$ until $42^{\circ}C$, and then at a rate of $1^{\circ}C \cdot min^{-1}$ until $44^{\circ}C$. Probe temperature was maintained at $44^{\circ}C$ until a stable LDF plateau had been reached representing physiological maximal flux (42, 108, 110), at which point the experiment was completed. During the maximal flux portion, \bar{T}_{exp} and \bar{T}_{con} were $\sim 34^{\circ}C$.

4.3.2 Physiological Variables

Heart rate (HR) was continuously obtained from R-R intervals using a 3-lead electrocardiogram (Bio Amp, ADInstruments, Colorado Springs CO, USA) and calculated using Lab Chart (version 8, ADInstruments). Blood pressure was recorded at the left ankle (5) before and after the normo- and hyper-thermic assessment using a manual sphygmomanometer. The ankle was used as a substitute for the arm as we did not want to occlude blood flow to the forearm and cause a reactive hyperemic response (77) at the site of SkBF measurement. Mean arterial pressure (MAP) was calculated using the following equation for normo- and hyper-thermia:

$$\text{MAP} = (0.66 \cdot \text{Diastolic Blood Pressure}) + (0.33 \cdot \text{Systolic Blood Pressure})$$

4.4 Data Processing

Laser-Doppler (SkBF and Probe temperature) and temperature (T_{re} , \bar{T}_{sk} , \bar{T}_{exp} , and \bar{T}_{con}) data were collected at 40 Hz and ECG at 1 kHz (PowerLab, ADInstruments), respectively, and stored on a personal computer to be analyzed and processed offline using Lab Chart (version 8, ADInstruments). Laser-Doppler data had a time-constant of 0.1 s and were used to calculate CVC by dividing LDF (PU) by calculated MAP (mmHg) for both normo- and hyper-thermia.

Data were then normalized to maximum CVC and expressed as percentage of maximum CVC (CVC%_{max}). Data from the ‘A’ manipulations were obtained from the lowest 30 s of LDF data, while data from the ‘B’ manipulations were taken as the highest 30 s peak of LDF. Maximal flux was obtained from the highest 5 min stable plateau.

LDF data were prepared for wavelet analysis with a custom written MATLAB® (The Mathworks, Inc., Natick, MA, USA) code. Data were detrended using a third-order polynomial, and bandpassed filtered between 0.0045 and 2.5 Hz.

4.5 Statistical Analysis

Data were normally distributed as assessed by Q-Q plots, skewness and kurtosis measures. Normality was defined as skewness less than ± 3 and kurtosis less than ± 9 . Results are presented in mean \pm S.E.M. Data collected were analyzed with a 2-way (core x time) repeated measures analysis of variance (ANOVA) for the control and experimental arm. Bonferroni *post-hoc* corrections were performed to test multiple comparisons. Paired samples *t*-tests were performed to test significant main effects at specific time points. Orthogonal polynomials were used to compare trends (linear, quadratic, and cubic) in the means of CVC, LDF, \bar{T}_{exp} , T_{re} and \bar{T}_{sk} during normo-compared with hyper-thermia.

Skin vasomotion data were assessed with spectral analysis of the LDF signal. Paired samples *t*-tests were performed on seven frequency bands were analyzed for the control arm between normothermia and hyperthermia: 0.0095 – 0.02 Hz, 0.005 – 0.01 Hz, 0.01 – 0.02 Hz, 0.02 – 0.05 Hz, 0.05 – 0.15 Hz, 0.15 – 0.4 Hz, 0.4 – 2.0 Hz. Paired-samples *t*-tests were performed between each frequency domain between normo- and hyper-thermia. The frequency spectrum was analyzed in five intervals for the experimental arm: 0.0095 – 0.02 Hz, 0.02 – 0.05 Hz, 0.05 – 0.15 Hz, 0.15 – 0.4 Hz, 0.4 – 2.0 Hz. Two-way (core x time) repeated measures ANOVAs were performed of each frequency interval between the four time points (A1, B1, A2, and B2). Bonferroni *post-hoc* corrections were performed to test multiple comparisons. Paired-samples *t*-tests were

performed between each frequency domain between normo- and hyper-thermia for each T_{loc} manipulation.

All statistical analyses were performed with SPSS (version 20, SPSS, Chicago, IL, USA). Complex interactions were explored using orthogonal polynomials to evaluate trends within the data. The level of significance was set to $p < 0.05$, with exception to the *post-hoc* testing as a Bonferroni adjustment was applied.

CHAPTER FIVE: RESULTS

5.1 Thermal Manipulations

The thermal protocol was successful in eliciting the desired manipulations of local and whole-body temperature (Fig. 10; bottom panel). During normothermia, T_{re} and \bar{T}_{sk} were $37.0 \pm 0.1^\circ\text{C}$ and $33.5 \pm 0.1^\circ\text{C}$, respectively. After the completion of normothermia, participants were passively heated for 95 ± 7 min to achieve a $\sim 1.0 \pm 0.1^\circ\text{C}$ rise in T_{re} . Hyperthermia measures were then performed with T_{re} and \bar{T}_{sk} at $38.1 \pm 0.1^\circ\text{C}$ and $38.4 \pm 0.3^\circ\text{C}$, respectively (both $p < 0.001$ vs. normothermia).

Control arm temperature (\bar{T}_{con}) decreased ($33.3 \pm 0.1^\circ\text{C}$) throughout normothermia ($p = 0.010$). See Table 4 for detailed \bar{T}_{con} and experimental arm temperature (\bar{T}_{exp}) throughout the measurement periods. \bar{T}_{exp} was significantly higher during the ‘B’ manipulations compared to the ‘A’ manipulations. Time to increase \bar{T}_{exp} from the ‘A’ to ‘B’ manipulations ranged from 30 – 160 s, whereas to decrease from the ‘B’ to ‘A’ manipulations took between 46 – 156 s, with each phase lasting between 270 – 360 s.

HR and MAP increased from 62 ± 3 beats $\cdot\text{min}^{-1}$ and 86 ± 1 mm Hg during normothermia, to 103 ± 5 beats $\cdot\text{min}^{-1}$ and 94 ± 2 mm Hg (both $p < 0.001$ vs. normothermia) during hyperthermia.

Table 4. Temperature of the control (\bar{T}_{con}) and experimental (\bar{T}_{exp}) forearms during local temperature manipulations during normothermia and hyperthermia ($\Delta T_{\text{re}} +1.1^{\circ}\text{C}$). Significant differences are within the same arm and core temperature phase. ^aSignificantly different than normothermic A1 ($p < 0.05$). ^bSignificantly different from normothermic B1 ($p < 0.05$). ^cSignificantly different than normothermic A2 ($p < 0.05$). ^dSignificantly different than hyperthermic B1 ($p < 0.05$). ^eSignificantly different than hyperthermic A1 ($p < 0.05$). ^fSignificantly different than hyperthermic B2 ($p < 0.05$).

	Normothermia				Hyperthermia			
	A1	B1	A2	B2	B1	A1	B2	A2
\bar{T}_{con}	33.3 ± 0.1	33.2 ± 0.1	33.2 ± 0.1	$33.0 \pm 0.1^{\text{a}}$	33.1 ± 0.1	33.0 ± 0.1	33.0 ± 0.1	33.1 ± 0.1
\bar{T}_{exp}	33.2 ± 0.1	$38.3 \pm 0.1^{\text{a}}$	$32.5 \pm 0.2^{\text{b}}$	$38.8 \pm 0.1^{\text{abc}}$	38.6 ± 0.1	$33.4 \pm 0.1^{\text{d}}$	$38.7 \pm 0.1^{\text{e}}$	$33.2 \pm 0.1^{\text{df}}$

the hot (38.5°C) \bar{T}_{exp} manipulation. The bottom panel has \bar{T}_{exp} (*open circles*), control (*filled circles*; \bar{T}_{con}), mean skin (*open upward triangles*; \bar{T}_{sk}), and core (*filled downward triangles*; T_{re}) temperature responses to local and whole-body temperature manipulations.

5.2 Local Temperature Effects During Normothermia on Skin Blood Flow

5.2.1 Laser-Doppler Flowmetry (PU)

During normothermia, LDF data of the experimental arm changed with each T_{loc} manipulation ($p < 0.001$), whereas control arm LDF data remained constant ($p = 0.148$). See Table 5 for LDF data of the experimental and control arm during each measurement phase throughout normothermia.

Table 5. Laser-Doppler flowmetry units (PU) for the experimental and control arm responding to local temperature changes during normothermia. ^aSignificantly different from A1 ($p < 0.05$). ^bSignificantly different from B1 ($p < 0.05$). ^cSignificantly different from A2 ($p < 0.05$).

	Experimental				Control			
	A1	B1	A2	B2	A1	B1	A2	B2
LDF (PU)	10.8	53.3	18.7	45.6	7.3	8.3	8.2	8.7
	± 0.7	$\pm 3.5^a$	$\pm 2.9^b$	$\pm 4.6^{ac}$	± 0.8	± 1.4	± 1.4	± 1.2

The $\Delta\text{PU}_{\text{exp}}$ (Fig. 11B) from A1 to B1 was $+42.5 \pm 3.8$ PU. Decreasing \bar{T}_{exp} from B1 to A2, $\Delta\text{PU}_{\text{exp}}$ was -34.6 ± 4.8 PU ($p < 0.001$). Finally, increasing \bar{T}_{exp} from A2 to B2, $\Delta\text{PU}_{\text{exp}}$ was $+26.9 \pm 3.4$ PU ($p = 0.002$ vs. A1 to B1, $p < 0.001$ vs. B1 to A2).

5.2.2 Cutaneous Vascular Conductance (%max)

During normothermia, CVC of the experimental arm changed with each T_{loc} manipulation ($p < 0.001$), whereas it remained constant for the control arm ($p = 0.172$).

See Table 6 for CVC data of the experimental and control arm during each measurement phase throughout normothermia.

Table 6. Cutaneous vascular conductance (CVC) expressed as percent of maximum for the experimental and control arm during normothermia in response to local temperature manipulations. ^aSignificantly different from A1 ($p < 0.05$). ^bSignificantly different from B1 ($p < 0.05$). ^cSignificantly different from A2 ($p < 0.05$).

	Experimental				Control			
	A1	B1	A2	B2	A1	B1	A2	B2
CVC (%max)	10.8 ±1.6	51.3 ±6.6 ^a	18.2 ±3.3 ^b	43.6 ±6.1 ^{ac}	8.5 ±1.1	9.6 ±1.6	9.4 ±1.6	10.1 ±1.4

The $\Delta\text{CVC}_{\text{exp}}$ (Fig. 11A) from A1 to B1 was $+40.5 \pm 5.6$ %max. Decreasing \bar{T}_{exp} from B1 to A2, $\Delta\text{CVC}_{\text{exp}}$ was -33.1 ± 5.9 %max ($p < 0.001$). Finally, increasing \bar{T}_{exp} from A2 to B2, $\Delta\text{CVC}_{\text{exp}}$ was $+25.4 \pm 4.0$ %max ($p = 0.002$ vs. A1 to B1, $p < 0.001$ vs. B1 to A2).

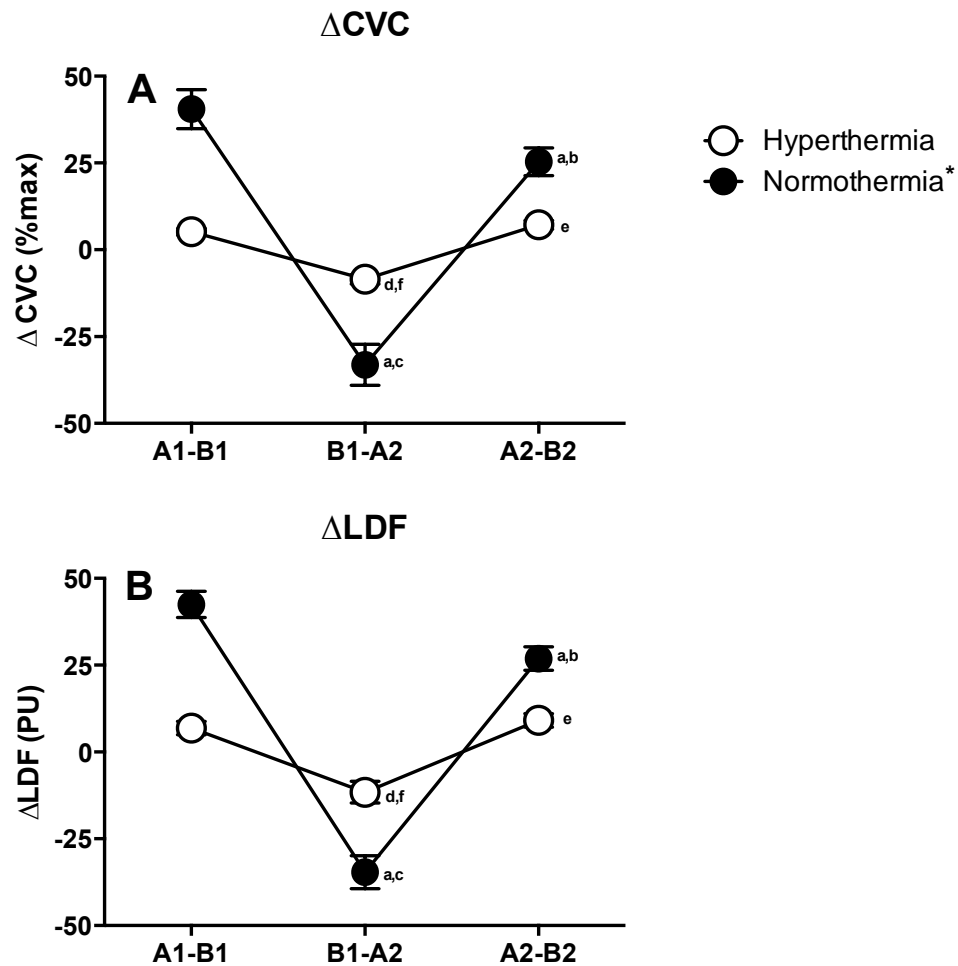


Figure 11. Changes to CVC (A) and LDF (B) from T_{loc} manipulations during normo- (filled circles) and hyper-thermia (open circles). *Significantly different from hyperthermic measures ($p < 0.05$). ^aSignificantly different from A1-B1 ($p < 0.05$). ^bSignificantly different from B1-A2 ($p < 0.05$). ^cSignificantly different from A2-B2 ($p < 0.05$).

5.3 Local Temperature Effects During Hyperthermia on Skin Blood Flow

5.3.1 Laser-Doppler Flowmetry (PU)

During hyperthermia, LDF data of the experimental arm ($p < 0.001$) changed with each T_{loc} manipulation, whereas control arm LDF data decreased ($p = 0.001$). See Table 7

for LDF data of the experimental and control arm during each measurement phase throughout hyperthermia.

Table 7. Laser-Doppler units (PU) for the experimental and control arm during hyperthermia in response to local temperature manipulations. ^aSignificantly different from B1 ($p < 0.05$). ^bSignificantly different from A1 ($p < 0.05$). ^cSignificantly different from B2 ($p < 0.05$).

	Experimental				Control			
	B1	A1	B2	A2	B1	A1	B2	A2
LDF (PU)	78.5 ±11.9	71.7 ±10.3 ^a	76.0 ±10.7 ^b	66.9 ±9.1 ^{abc}	48.1 ±4.5	44.7 ±3.8 ^a	46.8 ±4.0 ^b	44.0 ±3.5 ^{ac}

$\Delta\text{PU}_{\text{exp}}$ (Fig. 11B) during hyperthermia are presented in the same order as normothermia (A1 to B1, B1 to A2, and A2 to B2). $\Delta\text{PU}_{\text{exp}}$ between A1 and B1 was $+6.8 \pm 1.9$ PU. $\Delta\text{PU}_{\text{exp}}$ between B1 and A2 was -11.6 ± 3.1 PU ($p = 0.015$). Finally, $\Delta\text{PU}_{\text{exp}}$ concerning A2 and B2 was $+9.1 \pm 1.9$ PU ($p = 0.064$ vs. A1 to B1 $p = 0.007$ vs. B1 to A2).

$\Delta\text{PU}_{\text{exp}}$ between A1 and B1 during normothermia was 35.7 ± 3.9 PU greater ($p < 0.001$) than hyperthermia. The $\Delta\text{PU}_{\text{exp}}$ between B1 to A2 during normothermia was greater than hyperthermia (-23.0 ± 4.8 PU; $p = 0.001$). The final $\Delta\text{PU}_{\text{exp}}$ between A2 to B2 was 17.8 ± 3.8 PU greater ($p = 0.001$) than hyperthermia.

5.3.2 Cutaneous Vascular Conductance (%max)

During hyperthermia, CVC of the experimental arm ($p < 0.001$) changed with each T_{loc} manipulation, whereas it remained constant for the control arm ($p = 0.001$). See Table 8 for CVC data of the experimental and control arm during each measurement phase throughout hyperthermia.

Table 8. Cutaneous vascular conductance (CVC) expressed as a percent of maximum for the experimental and control arm during hyperthermia in response to local temperature manipulations. ^aSignificantly different from B1 ($p < 0.05$). ^bSignificantly different from A1 ($p < 0.05$). ^cSignificantly different from B2 ($p < 0.05$).

	Experimental				Control			
	B1	A1	B2	A2	B1	A1	B2	A2
CVC (%max)	61.9 ± 5.6	56.7 ± 5.0 ^a	60.6 ± 5.1	53.4 ± 4.7 ^{abc}	50.8 ± 5.1	47.1 ± 4.2 ^a	49.3 ± 4.5 ^b	46.5 ± 4.2 ^{ac}

$\Delta\text{CVC}_{\text{exp}}$ (Fig. 11) during hyperthermia are presented in the same order as normothermia (A1 to B1, B1 to A2, and A2 to B2). $\Delta\text{CVC}_{\text{exp}}$ between A1 and B1 was $+5.2 \pm 1.0$ %max. $\Delta\text{CVC}_{\text{exp}}$ between B1 and A2 was -8.5 ± 1.4 %max ($p = 0.001$). Finally, $\Delta\text{CVC}_{\text{exp}}$ concerning A2 and B2 was $+7.2 \pm 1.3$ %max ($p = 0.186$ vs A1 to B1 $p < 0.001$ vs B1 to A2).

$\Delta\text{CVC}_{\text{exp}}$ between A1 and B1 during normothermia was 35.3 ± 5.6 %max greater ($p < 0.001$) than hyperthermia. The $\Delta\text{CVC}_{\text{exp}}$ between B1 to A2 during normothermia was greater than hyperthermia (-24.7 ± 6.0 %max; $p = 0.003$). The final $\Delta\text{CVC}_{\text{exp}}$ between A2 to B2 was 18.2 ± 3.7 %max greater ($p = 0.001$) than hyperthermia.

5.3.3 Polynomial Contrasts

A linear trend component accounted for the greatest amount of the variance during normothermic assessment for T_{re} (95.65%), whereas a quadratic trend component explained most of the variance for \bar{T}_{sk} (92.31%). \bar{T}_{exp} variance during normothermia was explained by cubic (80.82%) and linear (18.24%) trend components. Likewise, the variance accounting for CVC_{exp} was explained by cubic (76.46%) and linear (18.55%)

trend components. As both CVC_{exp} and \bar{T}_{exp} were explained with similar linear and cubic trends, one can infer that CVC_{exp} is closely related to \bar{T}_{exp} during normothermia.

Table 9. Polynomial trend components between normo- and hyper-thermic assessment. During normothermia, the variance of the trend components explaining \bar{T}_{exp} was similar to the variance trend components of CVC_{exp} . However, during hyperthermia, the variance explaining CVC_{exp} was not similar to any other trend component specifically.

	Normothermia (VAR(p -value))				Hyperthermia (VAR(p -value))			
	T_c	\bar{T}_{sk}	\bar{T}_{exp}	CVC_{exp}	T_c	\bar{T}_{sk}	\bar{T}_{exp}	CVC_{exp}
Linear	96% (0.006)	0.38% (0.965)	18.24% (<0.001)	18.25% (0.002)	97.82% (0.002)	84.62% (0.367)	20.89% (<0.001)	51.72% (0.001)
Quadratic	0.0% (0.591)	92.31% (0.089)	0.94% (<0.001)	4.99% (0.001)	0.0% (0.343)	0.0% (0.780)	0.07% (0.140)	2.35% (0.060)
Cubic	0.0% (0.468)	0.0% (0.604)	80.82% (<0.001)	76.49% (<0.001)	1.75% (0.121)	7.69% (0.610)	79.04% (<0.001)	45.93% (0.001)

A linear trend component accounted for the greatest amount of the variance during hyperthermic assessment of T_{re} (97.82%) and \bar{T}_{sk} (84.62%). The variance explaining CVC_{exp} during hyperthermic assessment was explained by linear (51.72%), cubic (45.93%) and quadratic (2.35%) trend components. Since CVC_{exp} and \bar{T}_{exp} were not similar, as they were during normothermia, it can be inferred that the linear trends composing T_{re} or \bar{T}_{sk} influenced CVC_{exp} .

5.4 Wavelet Analysis

See Table 10 for the power spectra for the wavelet analysis of the control arm during normo- and hyper-thermia. Analysis of the vasomotion data of the control arm revealed no differences in the frequencies associated with endothelial ($p = 0.714$), NO-

independent ($p = 0.245$), NO-dependent ($p = 0.825$), neurogenic ($p = 0.863$) and cardiac ($p = 0.359$) function between normo- and hyper-thermia. Frequency domains associated with myogenic ($p = 0.034$) and respiratory ($p = 0.017$) function increased from normo- to hyper-thermia.

See Table 11 for the power spectra of the experimental arm during normo- and hyper-thermia during each temperature manipulation. Analysis of the vasomotion data of the experimental arm during normo- or hyper-thermia revealed no significant differences for the frequencies domains associated with endothelial, neurogenic, or cardiac function, or the myogenic frequency band during hyperthermia. During normothermia, the A1 manipulation was significantly less than B1 ($p < 0.001$), A2 ($p < 0.001$), and B2 ($p = 0.006$) for the myogenic band, and A1 was significantly less than B1 ($p = 0.036$) and B2 ($p = 0.015$) for the respiratory band. During hyperthermia only the respiratory frequency band had the A2 manipulation less than the B1 manipulation ($p = 0.045$).

Table 10. Spectral analysis of the control arm during normo- and hyper-thermic assessment. Data are presented as mean \pm S.E.M. ^aEndothelial band divided into two subsections. ^bSignificantly different from normothermia ($p < 0.050$).

Physiological function	Frequency interval (Hz)	Wavelet Transform (AU)	
		Normothermia	Hyperthermia
Endothelial	0.0095 – 0.02	0.241 \pm 0.063	0.275 \pm 0.062
NO-Independent ^a	0.005 – 0.01 ^a	0.154 \pm 0.034	0.222 \pm 0.036
NO-Dependent ^a	0.01 – 0.02 ^a	0.256 \pm 0.072	0.278 \pm 0.064
Neurogenic	0.02 – 0.05	0.343 \pm 0.052	0.354 \pm 0.035
Myogenic	0.05 – 0.15	0.504 \pm 0.092	0.857 \pm 0.115 ^b
Respiratory	0.15 – 0.6	0.414 \pm 0.092	0.738 \pm 0.099 ^b
Cardiac	0.6 – 2.0	0.610 \pm 0.142	0.786 \pm 0.119

Table 11. Spectral analysis of the experimental arm during each temperature manipulation during normo- and hyper-thermic assessment.^aSignificantly different from A1 ($p < 0.050$). ^bSignificantly greater from B1 ($p < 0.050$). ^cSignificantly different from normothermia ($p < 0.050$).

Physiological Function	Frequency interval (Hz)	Normothermia (AU)				Hyperthermia (AU)			
		A1	B1	A2	B2	B1	A1	B2	A2
Endothelial	0.0095 – 0.02	0.296 ±0.088	0.647 ±0.125	0.376 ±0.057	0.377 ±0.067	0.483 ±0.235	0.285 ±0.037	0.212 ±0.029 ^c	0.213 ±0.023 ^c
Neurogenic	0.02 – 0.05	0.508 ±0.183	0.692 ±0.214	0.680 ±0.286	0.827 ±0.344	0.446 ±0.068	0.507 ±0.104	0.369 ±0.078	0.327 ±0.045
Myogenic	0.05 – 0.15	0.282 ±0.028	0.631 ±0.054 ^a	0.708 ±0.063 ^a	0.762 ±0.109 ^a	0.906 ±0.188	0.751 ±0.112 ^c	0.751 ±0.149	0.681 ±0.102
Respiratory	0.15 – 0.6	0.217 ±0.039	0.472 ±0.069 ^a	0.431 ±0.096	0.514 ±0.075 ^a	0.775 ±0.130 ^c	0.681 ±0.112 ^c	0.746 ±0.170	0.594 ±0.115 ^{b,c}
Cardiac	0.6 – 2.0	0.310 ±0.067	0.673 ±0.096	0.526 ±0.078	0.623 ±0.084	0.719 ±0.140	0.713 ±0.133 ^c	0.753 ±0.158	0.696 ±0.131

CHAPTER SIX: DISCUSSION

The primary objectives of this study were to isolate the contributions of T_{re} and T_{loc} on SkBF by manipulating normo- and hyper-thermia ($\Delta T_{re} +1.1^{\circ}\text{C}$) and examine the interaction between local and reflexive SkBF control. The unique aspect of this study were the A-B-A-B T_{loc} manipulations that occurred during two distinct core temperatures, which provided insight into the relationship between local and reflexive SkBF control mechanisms. The primary finding was that high core temperatures elicited strong vasodilation even in a limb where local skin temperature was clamped at thermoneutral (33°C) throughout the experiment (57). Overall, peripheral afferents drove forearm CVC during normothermia, whereas central afferents attenuated the effect of T_{loc} manipulations on forearm CVC during hyperthermia, suggesting that high T_{re} can override peripheral afferents. These data support that deviations in core temperatures (either hot or cold) have the ability to override peripheral afferents' control of many physiological variables (24, 29, 33, 57, 83, 109).

Hyperthermia elicited reflexive vasodilation equating to ~50% of maximal CVC in the control arm, suggesting that central afferents can override peripheral afferents governing forearm SkBF. T_{loc} of the control arm was maintained at thermoneutral to assess the isolated effect of high core temperatures, while minimizing the influence of local control mechanisms on forearm SkBF. Similarly, Johnson et al. (57) passively heated participants while clamping one arm at thermoneutral, and the other heated to 42.5°C by spraying water of the desired temperatures. Passive heat stress elicited vasodilation in the thermoneutral arm equal to- or slightly less than- the heated arm (57). The authors concluded that reflexive vasodilation still occurs in a thermoneutral limb,

and that there is not a synergistic effect from combining local heating with whole-body heating on forearm SkBF. The aforementioned study maintained thermoneutrality by spraying 32°C water on the forearm and assessed SkBF via plethysmography (57). Plethysmography is a discontinuous assessment of forearm blood flow and cannot distinguish between skin and muscle blood flow. The current study immersed the forearm into a tightly controlled water bath to create a more powerful heat sink than local spraying, which allowed us to maintain strict T_{loc} of the control arm throughout. We assessed forearm SkBF via laser-Doppler flowmetry, which is limited to the skin, not influenced by underlying tissue (96), and allowed for continuous assessment of SkBF. Therefore, the current findings expand the work from Johnson et al. (57) by using a more powerful heat sink than water spraying, and manipulating T_{loc} during normo- and hyperthermia to assess how local and reflexive control of SkBF interact opposed to maintaining constant T_{loc} .

Peripheral afferents drove forearm SkBF during normothermia, as increases in T_{loc} were followed by a subsequent increase in forearm CVC. Previous work during normothermia has shown similar responses, with comparable (3, 17) and higher (3, 57, 105, 116, 117) T_{loc} increases facilitating vasodilation. When the skin was locally heated during normothermia, CVC transiently increased to 40 – 50% of maximum, however, vasodilation did not last the duration of the manipulation (see section 6.2, Experimental Considerations, for further discussion about the transient nature of the vasodilation). Local heating induced vasodilation is mainly a product of eNOS (71) and EDHF (8), among other local factors (58, 59, 81). Rapid local heating ($+0.1^{\circ}\text{C}\cdot\text{s}^{-1}$) to 39°C produces a plateau approximately 50% of maximal CVC that is largely NO-dependent (17).

Therefore, the vasodilation in the experimental arm that was observed during normothermia was likely due to NO, however this speculation remains to be tested. Local control mechanisms rapidly adapt with temperature changes (11, 69, 81) to protect underlying structures and to resist systemic temperature fluctuations. Rapid responses to local skin heating from 40°C to 42°C (45, 69, 81) or to 44°C (11) demonstrate that the local vasculature is able to quickly adapt to protect itself. Thus, local control mechanisms can function without changes in T_c or \bar{T}_{sk} , suggesting the body is able to locally thermoregulate (13, 58, 112).

Previous investigations of the relationship between local and reflexive SkBF control have been limited in methodology, since no T_{loc} manipulations have occurred during hyperthermia to examine the interaction of local and reflexive control mechanisms governing forearm SkBF. It was shown that central afferents attenuate local control of forearm SkBF during hyperthermia, whereas peripheral afferents have greater influence during normothermia. The A-B-A-B T_{loc} manipulations had a significantly lower effect on forearm SkBF during whole-body hyperthermia, as demonstrated by decreased changes in CVC magnitude during hyper- compared to normo-thermia. The increased SkBF from reflexive vasodilation and the decreased magnitude of CVC changes at hyperthermia from the T_{loc} manipulations allow for the inference that high T_{re} attenuate local control mechanisms of SkBF. During heat stress, the body activates mechanisms to dissipate heat to the surrounding environment via conductive and evaporative pathways to limit heat gain (90, 111). Passive heating elicits cutaneous vasodilation to increase convective heat exchange with the environment (93, 111). Reflexive vasodilation occurs when T_{loc} remains thermoneutral (57, 105), however, we were the first to demonstrate

that this reflexive vasodilation attenuates the ability to locally control SkBF during hyperthermia via the A-B-A-B T_{loc} manipulations.

Studies that used liquid conditioned garments as a method to control \bar{T}_{sk} and T_{re} often leave the SkBF measurement site uncovered (46, 112, 113). If the thermal background of the measurement site is not controlled, SkBF may be affected by local control mechanisms (33, 97). During pilot work, we observed an increase in T_{loc} of the control arm once T_{re} began to rise, even though it was in a $\sim 33^{\circ}\text{C}$ water bath. Since ambient temperature ($22.0^{\circ}\text{C} - 23.3^{\circ}\text{C}$) was lower than the water temperature used for the control arm, the upward drift in T_{loc} was a result of warm blood being sent to the extremities from reflexive vasodilation (93). Therefore, T_{loc} is likely to drift upwards from passive heating if it is not tightly regulated. The current design allowed us to maintain strict control of T_{loc} by consistently adding cool water into the water bath to maintain T_{loc} at 33°C , ensuring that if vasodilation occurred, it would be from reflexive vasodilation and not be influenced by local mechanisms.

An unexpected observation was the increased MAP with passive heat stress from 86 ± 1 mm Hg during normothermia to 94 ± 2 mm Hg during hyperthermia. Previous work (22) has shown a reduction of MAP following passive heat stress, however, participants in the study were supine and blood pressure was measured at heart level via the brachial artery. By design, brachial artery blood pressure was not desirable as both arms were being used to assess SkBF and we did not want to initiate reactive hyperemia (77) from the occlusion. Participants sat semi-recumbent, which allowed the site of measurement on their arms to be approximately heart level. With participants seated

during heat stress, MAP has been shown to increase (83, 84, 109). The semi-upright posture of the participants was likely to activate baroreceptors and cause an increase in blood pressure (95). Blood pressure measurements were assessed at the ankle, which was approximately 25 cm below heart level, which likely increased pressure due to differences in hydrostatic pressures (95). Also, due to venous pooling in the legs from vasodilation, baroreceptors were possibly activated due to a lack of central blood volume (62).

6.1 Spectral Analysis

To our knowledge, changes to the power spectral density of SkBF from passive heating have not been previously investigated. Increases in power spectral density in the control arm from normo- to hyper-thermia were associated with myogenic and respiratory activity. Myogenic activity is a measure of the rhythmic oscillations that respond to changes in intra-arterial pressure (6, 103). During hyperthermia, reflexive vasodilation occurs increasing the amount of blood being sent to the extremities, which is represented via increased laser-Doppler units and increase amplitude in the laser-Doppler signal. Which are both responsible for the increased myogenic activity. The respiratory band is associated with changes in pressure that occur during breathing (6, 103). Although it was not measured, hyperthermic induced hyperpnea, occurs during passive heat stress (39) and the increase power in the respiratory band is likely a result of increased depth of breathing.

During normothermia, myogenic activity of the experimental arm increased following B1 and remained elevated throughout normothermic assessment. Again, this was likely due to the increase in SkBF during the 'B' manipulation and observing many

more oscillations (6, 103). Interestingly, spectral density of the signal remained elevated during A2 assessment even though CVC returned to near baseline levels. This may be a result of the arterioles having an increased rate of contraction from the previous B1 manipulation, despite the blood flow decrease during A2. Also, during normothermia, respiratory activity increased during B1 and B2. We did not measure breathing rate, but it is logical to assume that it may have risen with increasing T_{loc} to increase activity of this band (39). During hyperthermic assessment the respiratory band was lower during the last block (A2) compared to the first block (B1). Endothelial function was lower during B2 and A2 of hyper- compared to normo-thermia. This suggests that the increased CVC observed during hyperthermia was not locally mediated (76). It is speculated that hyperpnea occurred during hyperthermia and accounted towards the increased respiratory activity (39). In addition, the cardiac band appeared to be higher during hyperthermia; however, it did not reach statistical significance.

6.2 Conclusions

The current study sought to investigate the relative roles of T_c and T_{loc} on forearm SkBF during normo- and hyper-thermia, and how reflexive and local control mechanisms of forearm SkBF interact. Clamping T_{loc} of the control arm at thermoneutral throughout the experiment provided insight into reflexive vasodilation without being influenced by local control mechanisms. During passive heat stress, reflexive vasodilation occurred in the thermoneutral arm and supported previous findings (57) that reflexive vasodilation is able to occur in a thermoneutral background. To examine how reflexive and local control mechanisms interacted, T_{loc} of the experimental arm was manipulated during two distinct core temperature phases. Manipulating T_{loc} during normothermia significantly affected

CVC_{exp} as it mirrored changes to \bar{T}_{exp} . During hyperthermia, T_{loc} manipulations had significantly less effect on CVC_{exp} , suggesting that the mechanisms involved with reflexive vasodilation elicited from high T_{re} attenuate local control on SkBF. These data indicate that SkBF responds greater to T_{loc} changes during normo- compared to hyperthermia.

6.3 Experimental Considerations

A young and fit population (7 males and 3 females; 20 – 26 years old; 52.1 – 69.2 mL·kg⁻¹·min⁻¹) was used to determine how local and reflexive control mechanisms interact to govern forearm SkBF. We did not include adolescents as they demonstrate decreased sweating ability and increased SkBF compared to adults (28), (78, 94), or older adults as they have lower SkBF response to passive heat stress (47, 82). Aerobic fitness is directly related to the magnitude of the SkBF response to local heating (47). Therefore, our results may not be generalizable to less fit populations or those significantly older or younger than the studied population.

The vasodilatory responses of the experimental arm were transient during the ‘B’ manipulations ($T_{loc} = 38.5^{\circ}\text{C}$; i.e., vasodilation did not last the entire ‘B’ manipulation), and it has been demonstrated that local heating to higher temperatures elicits further vasodilation (3, 57, 105, 116, 117). Therefore, it is possible that local heating to 38.5°C was not severe enough to warrant vasodilation for the duration of local heating. The approximate rate of heating achieved in the current study was $\sim 3^{\circ}\text{C}\cdot\text{min}^{-1}$, which is commonly used throughout local heating protocols (25, 41, 42). This heating rate is characterized by an initial peak occurring within the first 5 min, succeeded by a brief portion of nadir, and then a prolonged plateau taking longer to establish (17, 58, 59). It is

possible that the transient vasodilatory response observed during normothermia was the initial peak and nadir portions of local heating, before the plateau began to establish.

Wavelet analysis was performed in order to gain a mechanistic understanding of what was facilitating vasodilation during normothermia, and what mechanisms were hindering local SkBF control during hyperthermia. Due to the transient nature of the vasodilatory response (only lasting 30 – 60 s) to the T_{loc} manipulations, we were unable to get reliable data using wavelet analysis. The reason for needing a prolonged period of time to analyse blood flow dynamics is that they are composed of slow moving, nonstationary components (6, 76, 103). The endothelial band is found as slow as 0.0095 Hz, taking ~105 s to complete one cycle. Recently this band has been further separated to a frequency of 0.005 Hz (76), taking 200 s to complete one oscillation. It has been suggested that 30 min is needed to accurately analyse this component of SkBF (75, 76). Since we were unable to attain stable laser-Doppler data during the T_{loc} manipulations, we were unable to reliably perform wavelet analysis, as we would be analysing less than one complete cycle for the slower components of SkBF.

6.4 Future Directions

To delineate whether the attenuated local control of SkBF was a function of elevated \bar{T}_{sk} or T_{re} , T_{loc} manipulations can be done during different levels of heat stress. At the onset of passive heating, there is a lag time between increasing \bar{T}_{sk} and the subsequent increase in T_{re} . If T_{loc} manipulations were to be performed during this time, it would delineate whether T_{re} or \bar{T}_{sk} is the force during heat stress that attenuates local control of SkBF, and how each of their respective control mechanisms interact. Also, mild heat stress ($\Delta T_{re} +0.5^{\circ}\text{C}$), which would be more indicative of a real world heat stress

from work, sporting events, or prolonged heat exposure, might demonstrate more local control providing insight to what type of relationship exists between local and reflexive control. If the observed decrease in local control of SkBF was a function of high T_{re} , this would determine if the decreased local control was a graded or an ‘all-or-none’ response.

The current study observed local temperature changes between neutral and hot T_{loc} while participants were normo- or hyper-thermic. Vasoconstriction during local heating has been demonstrated during lower-body negative pressure (57), but not during whole-body heat stress with local cooling. Local skin cooling could determine at which point during heat stress vasoconstrictor function becomes compromised. This study could be replicated with a focus on hypo- instead of hyper-thermia to determine if local heating can cause vasodilation during whole-body cold stress. This would provide insight into how the body protects core temperature from cold stress.

REFERENCES

1. **Addison PS.** *The Illustrated Wavelet Transform Handbook: Introductory Theory and Applications in Science, Engineering, Medicine and Finance.* Taylor & Francis, 2002.
2. **Anderson C, Andersson T, and Wardell K.** Changes in skin circulation after insertion of a microdialysis probe visualized by laser Doppler perfusion imaging. *J Invest Dermatol* 102: 807-811, 1994.
3. **Barcroft H, and Edholm OG.** The effect of temperature on blood flow and deep temperature in the human forearm. *J Physiol* 102: 5-20, 1943.
4. **Benedicic M, Bernjak A, Stefanovska A, and Bosnjak R.** Continuous wavelet transform of laser-Doppler signals from facial microcirculation reveals vasomotion asymmetry. *Microvasc Res* 74: 45-50, 2007.
5. **Block FE, and Schulte GT.** Ankle blood pressure measurement, an acceptable alternative to arm measurements. *Int J Clin Monit Comput* 13: 167-171, 1996.
6. **Bračič M, and Stefanovska A.** Wavelet-based analysis of human blood-flow dynamics. *Bull Math Biol* 60: 919-935, 1998.
7. **Bruch-Gerharz D, Ruzicka T, and Kolb-Bachofen V.** Nitric oxide in human skin: current status and future prospects. *J Invest Dermatol* 110: 1-7, 1998.
8. **Brunt VE, and Minson CT.** KCa channels and epoxyeicosatrienoic acids: major contributors to thermal hyperaemia in human skin. *J Physiol* 590: 3523-3534, 2012.
9. **Caldwell JN, Matsuda-Nakamura M, and Taylor NA.** Three-dimensional interactions of mean body and local skin temperatures in the control of hand and foot blood flows. *Eur J Appl Physiol* 114: 1679-1689, 2014.
10. **Cals-Grierson MM, and Ormerod AD.** Nitric oxide function in the skin. *Nitric Oxide* 10: 179-193, 2004.
11. **Carter SJ, and Hodges GJ.** Sensory and sympathetic nerve contributions to the cutaneous vasodilator response from a noxious heat stimulus. *Exp Physiol* 96: 1208-1217, 2011.
12. **Charkoudian N.** Mechanisms and modifiers of reflex induced cutaneous vasodilation and vasoconstriction in humans. *J Appl Physiol (1985)* 109: 1221-1228, 2010.
13. **Charkoudian N.** Optimizing heat dissipation for every environment: the cool ability of the skin to locally regulate sweating. *J Appl Physiol (1985)* 109: 1288-1289, 2010.
14. **Cheung SS.** *Advanced Environmental Exercise Physiology.* Human Kinetics, 2010.
15. **Cheung SS.** Responses of the hands and feet to cold exposure. *Temperature* 2: 105-120, 2015.
16. **Cheung SS, and Daanen HA.** Dynamic adaptation of the peripheral circulation to cold exposure. *Microcirculation* 19: 65-77, 2012.
17. **Choi PJ, Brunt VE, Fujii N, and Minson CT.** New approach to measure cutaneous microvascular function: an improved test of NO-mediated vasodilation by thermal hyperemia. *J Appl Physiol (1985)* 117: 277-283, 2014.

18. **Cohen J.** *Statistical Power Analysis for the Behavioral Sciences.* Taylor & Francis, 1988.
19. **Cooper KE, Edholm OG, and Mottram RF.** The blood flow in skin and muscle of the human forearm. *J Physiol* 128: 258-267, 1955.
20. **Cosentino F, and Luscher TF.** Tetrahydrobiopterin and endothelial nitric oxide synthase activity. *Cardiovasc Res* 43: 274-278, 1999.
21. **Crandall CG, and Gonzalez-Alonso J.** Cardiovascular function in the heat-stressed human. *Acta Physiol (Oxf)* 199: 407-423, 2010.
22. **Crandall CG, Johnson JM, Kosiba WA, and Kellogg DL.** Baroreceptor control of the cutaneous active vasodilator system. *J Appl Physiol (1985)* 81: 2192-2198, 1996.
23. **Daanen HA.** Finger cold-induced vasodilation: a review. *Eur J Appl Physiol* 89: 411-426, 2003.
24. **Daanen HA, and Ducharme MB.** Finger cold-induced vasodilation during mild hypothermia, hyperthermia and at thermoneutrality. *Aviat Space Environ Med* 70: 1206-1210, 1999.
25. **Del Pozzi AT, Carter SJ, Collins AB, and Hodges GJ.** The regional differences in the contribution of nitric oxide synthase to skin blood flow at forearm and lower leg sites in response to local skin warming. *Microvasc Res* 2013.
26. **Del Pozzi AT, and Hodges GJ.** Comparison of the noradrenergic sympathetic nerve contribution during local skin heating at forearm and leg sites in humans. *Eur J Appl Physiol* 115: 1155-1164, 2015.
27. **Edholm OG, Fox RH, and Macpherson RK.** Vasomotor control of the cutaneous blood vessels in the human forearm. *J Physiol* 139: 455-465, 1957.
28. **Falk B, Bar-Or O, and MacDougall JD.** Thermoregulatory responses of pre-, mid-, and late-pubertal boys to exercise in dry heat. *Med Sci Sports Exerc* 24: 688-694, 1992.
29. **Flouris AD, and Cheung SS.** Influence of thermal balance on cold-induced vasodilation. *J Appl Physiol (1985)* 106: 1264-1271, 2009.
30. **Flouris AD, and Cheung SS.** Thermal basis of finger blood flow adaptations during abrupt perturbations in thermal homeostasis. *Microcirculation* 18: 56-62, 2011.
31. **Flouris AD, Westwood DA, Mekjavic IB, and Cheung SS.** Effect of body temperature on cold induced vasodilation. *Eur J Appl Physiol* 104: 491-499, 2008.
32. **Fox R, and Edholm O.** Nervous control of the cutaneous circulation. *British medical bulletin* 19: 110-114, 1963.
33. **Frank SM, Raja SN, Bulcao CF, and Goldstein DS.** Relative contribution of core and cutaneous temperatures to thermal comfort and autonomic responses in humans. *J Appl Physiol (1985)* 86: 1588-1593, 1999.
34. **Gagnon D, Crandall CG, and Kenny GP.** Sex differences in postsynaptic sweating and cutaneous vasodilation. *J Appl Physiol (1985)* 114: 394-401, 2013.
35. **Geyer MJ, Jan Y-K, Brienza DM, and Boninger ML.** Using wavelet analysis to characterize the thermoregulatory mechanisms of sacral skin blood flow. *The Journal of Rehabilitation Research and Development* 41: 797, 2004.
36. **Gonzalez-Alonso J, Crandall CG, and Johnson JM.** The cardiovascular challenge of exercising in the heat. *J Physiol* 586: 45-53, 2008.

37. **Grant R, and Holling H.** Further observations on the vascular responses of the human limb to body warming; evidence for sympathetic vasodilator nerves in the normal subject. *Clin Sci* 3: 273-285, 1938.
38. **Haeusler G, Haefely W, and Huerlimann A.** On the mechanism of the adrenergic nerve blocking action of bretylium. *Naunyn Schmiedebergs Arch Pharmacol* 265: 260-277, 1969.
39. **Haldane JS.** The Influence of High Air Temperatures: No. 1. *J Hyg (Lond)* 5: 494-513, 1905.
40. **Hodges GJ, Chiu C, Kosiba WA, Zhao K, and Johnson JM.** The effect of microdialysis needle trauma on cutaneous vascular responses in humans. *J Appl Physiol (1985)* 106: 1112-1118, 2009.
41. **Hodges GJ, and Del Pozzi AT.** Noninvasive examination of endothelial, sympathetic, and myogenic contributions to regional differences in the human cutaneous microcirculation. *Microvasc Res* 93: 87-91, 2014.
42. **Hodges GJ, Del Pozzi AT, McGarr GW, Mallette MM, and Cheung SS.** The contribution of sensory nerves to cutaneous vasodilatation of the forearm and leg to local skin heating. *Eur J Appl Physiol* 2015.
43. **Hodges GJ, and Johnson JM.** Adrenergic control of the human cutaneous circulation. *Appl Physiol Nutr Metab* 34: 829-839, 2009.
44. **Hodges GJ, Kosiba WA, Zhao K, Alvarez GE, and Johnson JM.** The role of baseline in the cutaneous vasoconstrictor responses during combined local and whole body cooling in humans. *Am J Physiol Heart Circ Physiol* 293: H3187-3192, 2007.
45. **Hodges GJ, Kosiba WA, Zhao K, and Johnson JM.** The involvement of heating rate and vasoconstrictor nerves in the cutaneous vasodilator response to skin warming. *Am J Physiol Heart Circ Physiol* 296: H51-56, 2009.
46. **Hodges GJ, Kosiba WA, Zhao K, and Johnson JM.** The involvement of norepinephrine, neuropeptide Y, and nitric oxide in the cutaneous vasodilator response to local heating in humans. *J Appl Physiol (1985)* 105: 233-240, 2008.
47. **Hodges GJ, Sharp L, Clements RE, Goldspink DF, George KP, and Cable NT.** Influence of age, sex, and aerobic capacity on forearm and skin blood flow and vascular conductance. *Eur J Appl Physiol* 109: 1009-1015, 2010.
48. **Hodges GJ, and Sparks PA.** Contributions of endothelial nitric oxide synthase, noradrenaline, and neuropeptide Y to local warming-induced cutaneous vasodilatation in men. *Microvasc Res* 90: 128-134, 2013.
49. **Houghton BL, Meendering JR, Wong BJ, and Minson CT.** Nitric oxide and noradrenaline contribute to the temperature threshold of the axon reflex response to gradual local heating in human skin. *J Physiol* 572: 811-820, 2006.
50. **Iatsenko D, McClintock PV, and Stefanovska A.** Linear and synchrosqueezed time-frequency representations revisited. Part I: Overview, standards of use, related issues and algorithms. *arXiv preprint arXiv:13107215* 2013.
51. **Iatsenko D, McClintock PV, and Stefanovska A.** Nonlinear Mode Decomposition: a new noise-robust, adaptive decomposition method. *arXiv preprint arXiv:12075567* 2012.
52. **Jackson AS, and Pollock ML.** Generalized equations for predicting body density of men. *Br J Nutr* 40: 497-504, 1978.

53. **Jackson AS, Pollock ML, and Ward A.** Generalized equations for predicting body density of women. *Med Sci Sports Exerc* 12: 175-181, 1980.
54. **Jan YK, Struck BD, Foreman RD, and Robinson C.** Wavelet analysis of sacral skin blood flow oscillations to assess soft tissue viability in older adults. *Microvasc Res* 78: 162-168, 2009.
55. **Johnson JM.** Exercise in a hot environment: the skin circulation. *Scand J Med Sci Sports* 20 Suppl 3: 29-39, 2010.
56. **Johnson JM.** Nonthermoregulatory control of human skin blood flow. *J Appl Physiol* (1985) 61: 1613-1622, 1986.
57. **Johnson JM, Brengelmann GL, and Rowell LB.** Interactions between local and reflex influences on human forearm skin blood flow. *J Appl Physiol* (1985) 41: 826-831, 1976.
58. **Johnson JM, and Kellogg DL, Jr.** Local thermal control of the human cutaneous circulation. *J Appl Physiol* (1985) 109: 1229-1238, 2010.
59. **Johnson JM, Minson CT, and Kellogg DL, Jr.** Cutaneous vasodilator and vasoconstrictor mechanisms in temperature regulation. *Compr Physiol* 4: 33-89, 2014.
60. **Johnson JM, and Park MK.** Effect of upright exercise on threshold for cutaneous vasodilation and sweating. *J Appl Physiol Respir Environ Exerc Physiol* 50: 814-818, 1981.
61. **Johnson JM, Taylor WF, Shepherd AP, and Park MK.** Laser-Doppler measurement of skin blood flow: comparison with plethysmography. *J Appl Physiol Respir Environ Exerc Physiol* 56: 798-803, 1984.
62. **Kellogg DL, Johnson JM, and Kosiba WA.** Baroreflex control of the cutaneous active vasodilator system in humans. *Circulation Research* 66: 1420-1426, 1990.
63. **Kellogg DL, Jr.** In vivo mechanisms of cutaneous vasodilation and vasoconstriction in humans during thermoregulatory challenges. *J Appl Physiol* (1985) 100: 1709-1718, 2006.
64. **Kellogg DL, Jr., Crandall CG, Liu Y, Charkoudian N, and Johnson JM.** Nitric oxide and cutaneous active vasodilation during heat stress in humans. *J Appl Physiol* (1985) 85: 824-829, 1998.
65. **Kellogg DL, Jr., Johnson JM, Kenney WL, Pérgola PE, and Kosiba WA.** Mechanisms of control of skin blood flow during prolonged exercise in humans. *Am J Physiol* 265: H562-568, 1993.
66. **Kellogg DL, Jr., Johnson JM, and Kosiba WA.** Competition between cutaneous active vasoconstriction and active vasodilation during exercise in humans. *Am J Physiol* 261: H1184-1189, 1991.
67. **Kellogg DL, Jr., Johnson JM, and Kosiba WA.** Control of internal temperature threshold for active cutaneous vasodilation by dynamic exercise. *J Appl Physiol* (1985) 71: 2476-2482, 1991.
68. **Kellogg DL, Jr., Johnson JM, and Kosiba WA.** Selective abolition of adrenergic vasoconstrictor responses in skin by local iontophoresis of bretylium. *Am J Physiol* 257: H1599-1606, 1989.
69. **Kellogg DL, Jr., Liu Y, Kosiba IF, and O'Donnell D.** Role of nitric oxide in the vascular effects of local warming of the skin in humans. *J Appl Physiol* (1985) 86: 1185-1190, 1999.

70. **Kellogg DL, Jr., Pérgola PE, Piest KL, Kosiba WA, Crandall CG, Grossmann M, and Johnson JM.** Cutaneous active vasodilation in humans is mediated by cholinergic nerve cotransmission. *Circ Res* 77: 1222-1228, 1995.
71. **Kellogg DL, Jr., Zhao JL, and Wu Y.** Endothelial nitric oxide synthase control mechanisms in the cutaneous vasculature of humans in vivo. *Am J Physiol Heart Circ Physiol* 295: H123-129, 2008.
72. **Kellogg DL, Jr., Zhao JL, and Wu Y.** Neuronal nitric oxide synthase control mechanisms in the cutaneous vasculature of humans in vivo. *J Physiol* 586: 847-857, 2008.
73. **Kellogg DL, Jr., Zhao JL, and Wu Y.** Roles of nitric oxide synthase isoforms in cutaneous vasodilation induced by local warming of the skin and whole body heat stress in humans. *J Appl Physiol (1985)* 107: 1438-1444, 2009.
74. **Kenny GP, Jay O, and Journey WS.** Disturbance of thermal homeostasis following dynamic exercise. *Appl Physiol Nutr Metab* 32: 818-831, 2007.
75. **Kvandal P, Landsverk SA, Bernjak A, Stefanovska A, Kvernmo HD, and Kirkeboen KA.** Low-frequency oscillations of the laser Doppler perfusion signal in human skin. *Microvasc Res* 72: 120-127, 2006.
76. **Kvandal P, Stefanovska A, Veber M, Désirée Kvermmo H, and Arvid Kirkeboen K.** Regulation of human cutaneous circulation evaluated by laser Doppler flowmetry, iontophoresis, and spectral analysis: importance of nitric oxide and prostaglandines. *Microvascular Research* 65: 160-171, 2003.
77. **Lewis T.** *The Blood Vessels of the Human Skin and Their Responses.* Classics of Medicine Library, 1927.
78. **Martin HL, Loomis JL, and Kenney WL.** Maximal skin vascular conductance in subjects aged 5-85 yr. *J Appl Physiol (1985)* 79: 297-301, 1995.
79. **McCord GR, Cracowski JL, and Minson CT.** Prostanoids contribute to cutaneous active vasodilation in humans. *Am J Physiol Regul Integr Comp Physiol* 291: R596-602, 2006.
80. **McLellan TM, Pope JI, Cain JB, and Cheung SS.** Effects of metabolic rate and ambient vapour pressure on heat strain in protective clothing. *Eur J Appl Physiol Occup Physiol* 74: 518-527, 1996.
81. **Minson CT, Berry LT, and Joyner MJ.** Nitric oxide and neurally mediated regulation of skin blood flow during local heating. *J Appl Physiol (1985)* 91: 1619-1626, 2001.
82. **Minson CT, Wladkowski SL, Cardell AF, Pawelczyk JA, and Kenney WL.** Age alters the cardiovascular response to direct passive heating. *J Appl Physiol (1985)* 84: 1323-1332, 1998.
83. **Morrison S, Sleivert GG, and Cheung SS.** Passive hyperthermia reduces voluntary activation and isometric force production. *Eur J Appl Physiol* 91: 729-736, 2004.
84. **Morrison SA, Sleivert GG, and Cheung S.** Aerobic influence on neuromuscular function and tolerance during passive hyperthermia. *Med Sci Sports Exerc* 38: 1754-1761, 2006.
85. **Noon JP, Walker BR, Hand MF, and Webb DJ.** Studies with iontophoretic administration of drugs to human dermal vessels in vivo: cholinergic vasodilatation is

mediated by dilator prostanoids rather than nitric oxide. *Br J Clin Pharmacol* 45: 545-550, 1998.

86. **Pérgola PE, Kellogg DL, Jr., Johnson JM, and Kosiba WA.** Reflex control of active cutaneous vasodilation by skin temperature in humans. *Am J Physiol* 266: H1979-1984, 1994.

87. **Rajan V, Varghese B, van Leeuwen TG, and Steenbergen W.** Review of methodological developments in laser Doppler flowmetry. *Lasers Med Sci* 24: 269-283, 2009.

88. **Ramanathan NL.** A new weighting system for mean surface temperature of the human body. *J Appl Physiol* 19: 531-533, 1964.

89. **Roddie IC, Shepherd JT, and Whelan RF.** The contribution of constrictor and dilator nerves to the skin vasodilatation during body heating. *J Physiol* 136: 489-497, 1957.

90. **Rowell LB.** Cardiovascular Adjustments to Thermal Stress. In: *Comprehensive Physiology* John Wiley & Sons, Inc., 2011.

91. **Rowell LB.** Human cardiovascular adjustments to exercise and thermal stress. *Physiol Rev* 54: 75-159, 1974.

92. **Rowell LB.** Neural control of muscle blood flow: importance during dynamic exercise. *Clin Exp Pharmacol Physiol* 24: 117-125, 1997.

93. **Rowell LB.** Reflex control of the cutaneous vasculature. *J Invest Dermatol* 69: 154-166, 1977.

94. **Rowland T.** Thermoregulation during exercise in the heat in children: old concepts revisited. *J Appl Physiol (1985)* 105: 718-724, 2008.

95. **Sagawa K.** Baroreflex Control of Systemic Arterial Pressure and Vascular Bed. In: *Comprehensive Physiology* John Wiley & Sons, Inc., 2011.

96. **Saumet JL, Kellogg DL, Jr., Taylor WF, and Johnson JM.** Cutaneous laser-Doppler flowmetry: influence of underlying muscle blood flow. *J Appl Physiol (1985)* 65: 478-481, 1988.

97. **Savage MV, and Brengelmann GL.** Control of skin blood flow in the neutral zone of human body temperature regulation. *J Appl Physiol (1985)* 80: 1249-1257, 1996.

98. **Sessler DI.** Thermoregulatory defense mechanisms. *Crit Care Med* 37: S203-210, 2009.

99. **Shastry S, Dietz NM, Halliwill JR, Reed AS, and Joyner MJ.** Effects of nitric oxide synthase inhibition on cutaneous vasodilation during body heating in humans. *J Appl Physiol (1985)* 85: 830-834, 1998.

100. **Shibasaki M, Wilson TE, Cui J, and Crandall CG.** Acetylcholine released from cholinergic nerves contributes to cutaneous vasodilation during heat stress. *J Appl Physiol (1985)* 93: 1947-1951, 2002.

101. **Soderstrom T, Stefanovska A, Veber M, and Svensson H.** Involvement of sympathetic nerve activity in skin blood flow oscillations in humans. *Am J Physiol Heart Circ Physiol* 284: H1638-1646, 2003.

102. **Stefanovska A.** Physics of the human cardiovascular system. *Contemporary Physics* 40: 31-55, 1999.

103. **Stefanovska A, Bračić M, and Kvernmo HD.** Wavelet analysis of oscillations in the peripheral blood circulation measured by laser Doppler technique. *IEEE Trans Biomed Eng* 46: 1230-1239, 1999.
104. **Tartas M, Bouye P, Koitka A, Jaquinandi V, Tan L, Saumet JL, and Abraham P.** Cathodal current-induced vasodilation to single application and the amplified response to repeated application in humans rely on aspirin-sensitive mechanisms. *J Appl Physiol (1985)* 99: 1538-1544, 2005.
105. **Taylor WF, Johnson JM, O'Leary D, and Park M, K.** Effect of high local temperature on reflex cutaneous vasodilation. *J Appl Physiol (1985)* 57: 191-196, 1984.
106. **Tesselaar E, and Sjoberg F.** Transdermal iontophoresis as an in-vivo technique for studying microvascular physiology. *Microvasc Res* 81: 88-96, 2011.
107. **Tew GA, Klonizakis M, Moss J, Ruddock AD, Saxton JM, and Hodges GJ.** Reproducibility of cutaneous thermal hyperaemia assessed by laser Doppler flowmetry in young and older adults. *Microvasc Res* 81: 177-182, 2011.
108. **Tew GA, Klonizakis M, Moss J, Ruddock AD, Saxton JM, and Hodges GJ.** Role of sensory nerves in the rapid cutaneous vasodilator response to local heating in young and older endurance-trained and untrained men. *Exp Physiol* 96: 163-170, 2011.
109. **Thomas MM, Cheung SS, Elder GC, and Sleivert GG.** Voluntary muscle activation is impaired by core temperature rather than local muscle temperature. *J Appl Physiol (1985)* 100: 1361-1369, 2006.
110. **Vionnet J, Calero-Romero I, Heim A, Rotaru C, Engelberger RP, Dischl B, Noel B, Liaudet L, Waeber B, and Feihl F.** No major impact of skin aging on the response of skin blood flow to a submaximal local thermal stimulus. *Microcirculation* 21: 730-737, 2014.
111. **Webb P.** The physiology of heat regulation. *Am J Physiol* 268: R838-850, 1995.
112. **Wingo JE, Low DA, Keller DM, Brothers RM, Shibasaki M, and Crandall CG.** Skin blood flow and local temperature independently modify sweat rate during passive heat stress in humans. *J Appl Physiol (1985)* 109: 1301-1306, 2010.
113. **Wong BJ.** Sensory nerves and nitric oxide contribute to reflex cutaneous vasodilation in humans. *Am J Physiol Regul Integr Comp Physiol* 304: R651-656, 2013.
114. **Wong BJ, and Fieger SM.** Transient receptor potential vanilloid type 1 channels contribute to reflex cutaneous vasodilation in humans. *J Appl Physiol (1985)* 112: 2037-2042, 2012.
115. **Wong BJ, and Fieger SM.** Transient receptor potential vanilloid type-1 (TRPV-1) channels contribute to cutaneous thermal hyperaemia in humans. *J Physiol* 588: 4317-4326, 2010.
116. **Wyss CR, Brengelmann GL, Johnson JM, Rowell LB, and Niederberger M.** Control of skin blood flow, sweating, and heart rate: role of skin vs. core temperature. *J Appl Physiol* 36: 726-733, 1974.
117. **Wyss CR, Brengelmann GL, Johnson JM, Rowell LB, and Silverstein D.** Altered control of skin blood flow at high skin and core temperatures. *J Appl Physiol* 38: 839-845, 1975.

APPENDIX A

Informed Consent:

Project Title: The isolated and synergistic effect of core body and skin temperature on forearm skin blood flow (EEL-093).

Principal Investigator:
Dr. Stephen Cheung, Ph.D. (Professor)
Department of Kinesiology
Brock University
905-688-5550 x 5662, scheung@brocku.ca

Principal Student Investigator:
Matthew Mallette (M.Sc. Candidate)
Department of Kinesiology
Brock University
905-688-5550 x 4901, mm09pk@brocku.ca

Co-Investigator
Dr. Gary Hodges, Ph.D. (Adjunct Professor)
Department of Kinesiology
Brock University
905-688-5550 x 4901, ghodges@brocku.ca

INVITATION

You are invited to participate in a study that involves research if you are a healthy male or female 18-35 years old. The purpose of this study is to examine the influence of whole body hyperthermia on skin blood flow when forearm temperature is hot (38.5°C) compared to when it is maintained in a thermoneutral state (33°C).

WHAT'S INVOLVED

There will be a total of two sessions. During the first session you will be screened for participation, provide anthropometric measurements, a treadmill $\text{VO}_{2\text{peak}}$ test, as well as be familiarized with the study's equipment. The second session will be experimental session.

At the familiarization session, you will have your height, weight, body fat, and aerobic fitness measured. Body fat testing will be performed using skinfold calipers, which might cause a slight pinching sensation, and will be taken by someone of the same sex in a private room. You will exercise on a motorized treadmill at a gradually increasing incline until exhaustion in order to obtain your peak oxygen uptake ($\text{VO}_{2\text{peak}}$) and maximum heart rate (HR_{max}). These tests will be used to describe the subject pool in published reports. Time for this session is about 1 hour.

At the start of the experimental session, you will change into a t-shirt and shorts. Following this, you will have your internal temperature measured by inserting a rectal temperature sensor as well as provide a urine sample to assess your hydration status. The rectal sensor consists of a very thin and flexible plastic tube that you insert 15 cm beyond the anus. Appropriate change rooms will be provided for you to change into the required clothing, and insert the rectal thermometer. Skin temperature will be monitored using sensors taped to ten sites on your body. A heart rate chest strap and watch will continuously monitor your heart rate. Your blood pressure will be measured throughout the experiment with a manual blood pressure cuff placed around your lower right leg (just above the ankle). You will be asked remove your shirt (females will be asked to wear a sports bra) and will be instrumented with a heart rate strap and skin thermistors before putting on a liquid conditioning garment (LCG), which is similar to a diving wet suit lined with flexible PVC tubing throughout. The garment consists of a pair of pants, jacket, and hood, leaving the face, hands, forearms and feet uncovered. During the experiments, warm (49°C) water will be run through the tubing to raise skin and core temperature. You will have a skin blood flow sensor attached with tape to each of your forearms.

During each session you will be asked to sit in a chair that has water troughs in place of arm rests. A baseline measurement will occur by sitting in the chair and the LCG will maintain a thermoneutral environment for ~20 minutes by circulating ~32°C water throughout the LCG until mean body skin temperature stabilizes at 33°C. A blood pressure measurement will be taken 20 minute intervals throughout the experimental session. This is similar to when a doctor takes blood pressure. Over the next 26 minutes, water temperature for one forearm will be rapidly changed between 33°C and 38.5°C in five minute intervals, and the other forearm will be kept at a constant temperature of 33°C. Blood pressure measurements will be taken before and after each temperature manipulation. Then warm water (49°C) will be pumped through the LCG to increase your core temperature by 1.2°C. The temperature of the water in the LCG will then be adjusted to keep your core temperature stable. Again, over the next 26 minutes, skin temperature of one forearm will be rapidly changed between 38.5°C and 33°C in five minute intervals, and the other forearm will be kept at a constant temperature of 33°C. Following this last forearm temperature manipulation, skin temperature of the areas under the laser-Doppler probe will be raised to 44°C for ten minutes in order to elicit a maximal skin blood flow response. You will be asked to remain in the laboratory for 30 minutes to ensure that you are symptom-free after the experiment has concluded. Total time commitment for the session is about 3.5 hours.

POTENTIAL BENEFITS AND RISKS

Possible benefits of participation include a free body composition test, normally costing \$50, and a free VO_{2peak} test, normally costing \$100 - \$150. You will also receive \$50 for participating in the experimental session.

There may be risks associated with participation. The exercise (VO_{2peak}) test is an “all-out” effort that is performed to exhaustion. You may feel quite tired for up to 48 h after the test. There is a very remote risk of heart attack or stroke when exercising to exhaustion, but this is minimized with the use of the health screening questionnaire, as well as the monitoring of HR during the test. There will be at least two investigators trained in First Aid and CPR present for each experiment. The investigators will contact you later the same day following each session to check on your health status, so we will need a current phone number to do so.

Experimental sessions will be terminated if:

1. Core temperature rises above 40.0°C.
2. Systolic blood pressure drops below 80 mmHg for more than 1 min.
3. You decide, for any reason, to end the experiment.
4. The investigators determine that you are unable/unfit to continue.

Hyperthermia

Symptoms that may be experienced with hyperthermia include: discomfort, sweating, flushing and redness in the face and body, thirst, loss of fine motor coordination due to sweating, minor mental confusion, dizziness, nausea and a drop in blood pressure. Given the level of hyperthermia employed in the proposed study (skin temperature of ~38.5°C, core temperature of ~38.2°C to 38.5°C), it is very unlikely that any serious symptoms would arise (as core temperature will not rise above 39.0°C). In event of intolerable symptoms, the heating protocol would be terminated immediately, followed by the circulation of cold water through the LCG, allowing for the rapid return of skin to normothermic levels. This typically removes most of any unpleasant feelings with the heating. Water will be available to you throughout. You will be in a reclined and seated position throughout the experiment, so there is no chance of you falling in the unlikely case that you become dizzy or faint.

Other Risks

The use of skin fold calipers may cause a slight pinching sensation. All skin fold measurements will be taken in a private room by an investigator of the same sex. The body sites for skin fold measurements are triceps, subscapula, mid-axilla, supra-iliac crest, chest, abdomen and thigh.

There is also a chance that surface temperature sensors or tape use with these sensors may cause some skin irritation, although this adverse response is rare. Alternative adhesive options are available if needed.

If you experience any unusual symptoms after completing a testing session, you should immediately seek medical attention and inform Dr. Cheung. The investigators will also contact you later the same day of your participation to ensure that you are in a healthy state. Depending on your health status, you may be asked to consult with a physician.

RECTAL PROBE

Insertion of the flexible rectal probe may cause slight discomfort. You will be given instruction about how to prepare the probe, and will self-insert the probe in a private room. You will be provided with water-based lubricant if necessary, and will secure the probe with a soft gauze “sumo sling” harness, which will keep it in place during the experiment.

When performed in a healthcare setting, insertion of the rectal probe is a controlled act as set out in the Regulated Health Professions Act. While this act does not extend to research outside of a healthcare setting, you should be aware of the following potential risks:

- Insertion of the rectal probe can stimulate the vagus nerve which can cause slowing of the heart rate which may lead to fainting. This is more likely to happen if you have a low resting heart rate.
- Perforation of the bowel can lead to peritonitis, a serious infection of the abdominal cavity, though the investigators are unaware of this ever occurring in a research setting.

You should not participate in this research if you are under the influence of alcohol or other sedating substances (tranquilizers, sleeping pills, street drugs) or have any history of fainting or heart disease.

CONFIDENTIALITY

Investigators will require disclosure of your name and contact information (phone, email), and therefore your participation is not anonymous during the conduct of the research. All participants will have their names removed from any data and a participant ID number used instead. The master list matching participants to data will be kept by the listed researchers, and will be destroyed following data collection and giving you your own and the group’s average results.

All information you provide is considered confidential; your name will not be included or, in any other way, associated with the data collected in the study. Furthermore, because our interest is in the average responses of the entire group of participants, you will not be identified individually in any way in written reports of this research.

VOLUNTARY PARTICIPATION

Participation in this study is voluntary. If you wish, you may decline to answer any questions or participate in any component of the study. Further, you may decide to withdraw from this study at any time and may do so without any penalty or loss of benefits to which you are entitled. This can be done in-person, through e-mail (Matt Mallette, mm09pk@brocku.ca; Dr. Stephen Cheung, scheung@brocku.ca) or through telephone (Dr. Stephen Cheung, 905-688-5550x5662). Participation, non-participation, or withdrawal from the study will not affect your standing at Brock University.

PUBLICATION OF RESULTS

Results of this study may be published in professional journals and presented at conferences, but your personal information and participation will remain confidential. Feedback about this study will be available from Dr. Stephen Cheung (scheung@brocku.ca, 905-688-5550x5662).

CONTACT INFORMATION AND ETHICS CLEARANCE

If you have any questions about this study or require further information, please contact the Principal Investigator using the contact information provided above. This study has been reviewed and received ethics clearance through the Research Ethics Board at Brock University (13-283). If you have any comments or concerns about your rights as a research participant, please contact the Research Ethics Office at (905) 688-5550 Ext. 3035, reb@brocku.ca.

CONSENT FORM**The isolated and synergistic effect of core body and skin temperature on forearm skin blood flow (EEL-093).**

I agree to participate in this study described above. I have made this decision based on the information I have read in this Informed Consent Letter. I have had the opportunity to receive any additional details I wanted about the study and understand that I may ask questions in the future. I understand that I may withdraw this consent at any time by telling or writing Drs. Cheung or Hodges or Mr. Mallette. My participation, non-participation, or withdrawal from the study will not affect my standing at Brock University.

Participant Name: _____

Participant Signature: _____ Date: _____

Principal Investigator: Stephen S. Cheung, Ph.D.

Principal Investigator Signature: _____ Date: _____

Thank you for your assistance in this project. Please keep a copy of this form for your records.

APPENDIX A

The isolated and synergistic effect of core body skin temperature and skin temperature on forearm skin blood flow (EEL-093)

Environmental Ergonomics Laboratory Fitness Screening Form

Please read over the questions below*. They are to assist in assessing whether you are fit to participate in this study. Please ask the investigators if you have any queries while filling out the form.

Screening Questions*	YES	NO
1. Has your doctor ever said that you have a heart condition and that you should only do physical activity recommended by a doctor?		
2. Do you feel pain in your chest when you do physical activity?		
3. In the past month, have you had chest pain when you were not doing physical activity?		
4. Do you lose your balance because of dizziness or do you ever lose consciousness?		
5. Do you have a bone or joint problem (for example, back, knee or hip) that could be made worse by a change in your physical activity?		
6. Is your doctor currently prescribing drugs (for example, water pills) for your blood pressure or heart condition?		
7. Do you know of any other reason why you should not do physical activity?		
8. Current pregnancy or menstrual irregularities (e.g., loss of cycle) in females?		
9. Do you have any bowel or prostate problems (e.g. colitis, irritable bowel syndrome, prostate problems)		
10. Neuromuscular (e.g., epilepsy, Multiple Sclerosis, Cerebral Palsy), skeletal (e.g., inflammatory or degenerative arthritis) or circulatory (e.g., diabetes, hypertension) disorders?		
11. Do you have a tendency for, or ever been diagnosed with, claustrophobia (a very strong fear of confined spaces)?		

Name: _____

Signature _____

Date** _____